

Energy-Efficient Algorithms for Target Monitoring in Mobile Sensor Networks

Walid Masoudimansour

A Thesis

in

the Department

of

Electrical and Computer Engineering

Presented in Partial Fulfillment of the Requirements

for the Degree of Master of Applied Science at

Concordia University

Montréal, Québec, Canada

May 2012

© Walid Masoudimansour, 2012

CONCORDIA UNIVERSITY
SCHOOL OF GRADUATE STUDIES

This is to certify that the thesis prepared

By: Walid Masoudimansour

Entitled: Energy-Efficient Algorithms for Target Monitoring in Mobile Sensor
 Networks

and submitted in partial fulfilment of the requirements for the degree of

Master of Applied Science

Complies with the regulations of this University and meets the accepted standards with respect to originality and quality.

Signed by the final examining committee:

_____ Dr. Rabin Raut, Chair

_____ Dr. Wenfang Xie (MIE), External

_____ Dr. M. Reza Soleymani, Examiner

_____ Dr. Amir G. Aghdam, Supervisor

Approved by: _____

Dr. W. E. Lynch, Chair

Department of Electrical and Computer Engineering

_____ 2012 _____

Dr. Robin A. L. Drew

Dean, Faculty of Engineering and Computer Science

ABSTRACT

Energy-Efficient Algorithms for Target Monitoring in Mobile Sensor Networks

Walid Masoudimansour

The main focus of this work is directed towards maximization of the lifetime of a network of cooperating mobile sensors monitoring a pre-specified target. It is assumed that the main sources of energy consumption in the network are movement, communication and sensing. It is desired to gather information about a moving target in a 2D field and find a proper route to transmit it to a fixed base or destination point. In order to find the most efficient route for transmitting information, the field is discretized as a grid of nodes. It is assumed that the sensors and target are located in the nodes at any point in time. A directed graph is subsequently constructed whose vertices are the grid nodes, and whose edges are weighted properly based on their residual energy. The proper set of nodes are then obtained (which form the desired route for maximizing the lifetime of the network) by solving the shortest path problem in the resultant graph. Finally, a proper model is adopted for the batteries to plan the sensor movement by solving a nonlinear programming problem to minimize the energy consumption of the overall network.

To my wife and my parents

ACKNOWLEDGEMENTS

This work would not be possible without the guidance and the help of several people. First and foremost, I would like to express my utmost gratitude to my supervisor, Dr. Amir G. Aghdam, for his continuous encouragement, help, support and inspiration.

I also, offer my sincerest appreciation to my colleague, Mr. Hamid Mahboubi, who contributed and extended his valuable assistance in the preparation and completion of this study. Deepest gratitude are also due to Dr. Jalal Habibi for the ideas, knowledge and experience he shared with me. Special thanks also to all my friends, especially group members.

TABLE OF CONTENTS

LIST OF FIGURES	viii
LIST OF ABBREVIATIONS AND SYMBOLS	x
1 Introduction	1
1.1 Motivation	1
1.2 Related Work	3
1.2.1 Network-Level Lifetime Maximization Approach	3
1.2.2 Sensor-Level Lifetime Maximization Approach	5
1.3 Thesis Contributions	7
1.4 Thesis Outline and Publications	8
2 Maximum Lifetime Strategy for Target Monitoring in Mobile Sensor Networks in Presence of Obstacles	10
2.1 Voronoi Partitioning	11
2.1.1 Conventional Voronoi Diagram	12
2.1.2 Energy-Based Voronoi Diagram	13
2.2 Problem Formulation	18
2.3 Proposed Algorithm	21
2.4 Simulation Results	37

2.5	Summary	42
3	Movement Planning with Respect to Battery Model for Lifetime Op- timization in Mobile Sensor Networks	44
3.1	Problem Statement	45
3.2	Proposed Strategy	46
3.3	Simulation Results	54
3.4	Summary	56
4	Conclusions and Future Work	58
4.1	Conclusions	58
4.2	Suggestions for Future Work	60
	Bibliography	62

LIST OF FIGURES

2.1	An example of a conventional Voronoi partitioning of a field which contains 10 nodes.	13
2.2	An example of the consumed energy Voronoi diagram for 2 sensors with different amounts of remaining energy.	16
2.3	An example of a sensor near an obstacle with blocked sensing capability .	16
2.4	An example of a sensor near an obstacle with blocked communication capability	17
2.5	An example of the obstructed energy-based Voronoi diagram for two sensors with different levels of remaining energy.	18
2.6	Edges originating from the target to the adjacent graph nodes for a sample consumed energy Voronoi diagram.	22
2.7	Different types of edges for a field with three sensors.	24
2.8	Snapshots of the network utilizing the proposed technique for 20 sensors in three different iterations.	38
2.9	Energy of the sensors during network lifetime: (a) tracking algorithm from [1]; (b) proposed algorithm.	40
2.10	Snapshots of the network configuration obtained by the proposed technique for 20 sensors in three different steps.	41

2.11	Energy of the sensors during network lifetime in presence of obstacles: (a) tracking algorithm from [1]; (b) proposed algorithm.	42
3.1	The two-well battery model	47
3.2	A sample movement/replenishing period in a planned sensor movement.	50
3.3	Movement profile of sensor in Example 1 for $n = 2$	55
3.4	Energy profile of sensor in Example 1 for $n = 2$	55
3.5	Energy profile of the sensor without movement planning in Example 2.	56
3.6	Energy profile of the sensor with movement planning in Example 2.	57

LIST OF ABBREVIATIONS

E-Voronoi	Energy-based Voronoi diagram
EC-Nearest	Nearest sensor to a node in terms of energy consumption
KBM	Kinetic battery model
MEMS	Microelectromechanical systems
MPAD	Mobility prediction-based adaptive data gathering
MSN	Mobile sensor network
OE-Voronoi	Obstructed energy-based Voronoi diagram

Chapter 1

Introduction

1.1 Motivation

Mobile sensor networks (MSN) have attracted considerable interest in recent years, due mainly to rapid technological advances in the fabrication of microelectromechanical systems (MEMS). Collaborative mobile sensors have been deployed effectively in different types of dynamic environments. The scalability and flexibility of such sensors make them suitable for a wide range of practical applications such as target tracking [2–6], health monitoring [7–10], intrusion detection [11–13], surveillance [14], environmental monitoring [15–19], and traffic control [20, 21], to name only a few. Minimizing the energy consumption of sensors in an MSN is an important problem which has been the focal point of extensive research in the past several years [6, 22, 23]. Note that each sensor

is typically equipped with a battery as its source of energy, and has three predominant energy loss mechanisms: movement, communication, and sensing. Therefore, for the design of an energy-efficient MSN it is important to develop a proper resource allocation strategy which takes these three sources of energy consumption into consideration.

Maximizing network lifetime is of utmost importance in an MSN, which is directly related to minimizing the energy consumption of the network. Network lifetime is one of the most important metrics for evaluating the performance of an MSN. It is to be noted that recharging or replacing the battery of a sensor in a network is a tedious process, which may not be feasible in many applications. A variety of definitions are given for network lifetime in the literature, the most common of which is the time it takes for the first sensor to completely deplete its energy [22, 24–27]. This is sometimes referred to as *n-of-n* lifetime [28].

The problem of lifetime maximization in an MSN can be addressed in two different ways: at the network level and at the sensor level. The former approach takes all components of the network into consideration, while the latter is concerned with the minimization of energy consumption of each individual sensor in the network. In both approaches, it is important to have a proper model of the battery, in order to formulate the energy consumption of the sensors for the underlying optimization problem.

1.2 Related Work

In this section, some of the existing results for network-level and sensor-level lifetime maximization in an MSN are reviewed.

1.2.1 Network-Level Lifetime Maximization Approach

Several network-level strategies have been proposed in the literature to improve the lifetime of a mobile sensor network.

In many cases, the sink node, which is usually the node with the highest energy consumption rate (as it processes the gathered data), is more likely to run out of battery first. Several techniques are developed in the literature to address this problem [23, 29–35]. For example, an optimal distributed information flow strategy is provided in [30] for a network consisting of battery-powered sensors and a mobile sink. In [36], the problem of energy imbalance in many-to-one sensor networks is investigated, and a general model is suggested for maximizing the network lifetime. An analytical framework is proposed in [37] for the coverage and lifetime of an MSN using a two-dimensional Gaussian distribution. Given the evolutionary nature of MSNs, it would be reasonable to use evolutionary approaches (such as genetic algorithms) to tackle some of the existing problems in this type of networks [38–42]. For instance, a hybrid approach is presented in [40], which is a combination of a genetic algorithm and schedule transition operations. The work aims at scheduling the operation of the sensors in the network by finding the

largest number of disjoint sets of sensors such that every set is able to completely cover the target area.

Energy-efficient algorithms for sensor networks can also be developed using dynamic programming [43–46]. For example, the authors in [44] use this technique for efficient routing in wireless sensor networks which does not have the shortcomings of the existing results in terms of energy imbalance. The method is used to address the demise of the sensor closer to the sink node, which is a common problem in many-to-one sensor networks. Given the information exchange between the sensors in order to achieve a global objective, neural network methods can also be very effective in developing energy-efficient strategies for this type of system [47–51]. As an example, a cluster-based routing algorithm is introduced in [50] which is based on Fuzzy-ART neural networks to prolong the lifetime of a sensor network.

Among the three main sources of energy consumption in an MSN discussed earlier, sensor movement is typically the most dominant one. Sensor movement planning for increased durability of the network has been extensively investigated in the literature. In [52], the problems of efficient routing and efficient mobility are considered simultaneously to develop a lifetime maximizing strategy for an MSN. To this end, the problem is formulated as a nonlinear nonconvex optimization, and is solved in a distributed fashion using a novel convergent algorithm. The lifetime maximization based only on the mobility of sensors is subsequently studied in [53]. Lifetime increasing in a

delay-tolerant MSN is addressed in [54] by proposing a mobility prediction-based adaptive data gathering protocol (MPAD) and using the random waypoint mobility model. In this protocol, a distributed decision-making strategy is utilized by sensors to replicate the messages and transmit them to the neighboring sensor nodes with a higher probability of meeting the sink node. Some of the shortcomings of the cluster-based routing protocols designed for an MSN are addressed in [55] by proposing a fault-tolerant clustering protocol. Some other works take advantage of the mobility capability of mobile nodes in a hybrid network consisting of static and mobile sensors for energy harvesting or recharge, and delivering energy to static nodes (e.g., see [56]).

1.2.2 Sensor-Level Lifetime Maximization Approach

In sensor-level lifetime maximization methods, each sensor is considered as an independent unit in the network. The objective is to increase the network lifetime by increasing the lifetime of every sensor in the network. In order to maximize the lifetime of a sensor it is important to use a sufficiently accurate model for the battery and a sufficiently accurate model for the energy consumption of the sensors (the latter is directly related to the sensors' actuators). Various battery models with different characteristics are proposed in the literature. Electromechanical models, for instance, utilize the chemical processes in a battery to model its behavior. These models are generally very accurate, at the cost of higher complexity [57, 58]. A model based on the electrical circuit elements and

their mathematical description is introduced in [59,60]. Stochastic models, on the other hand, use an abstract method to formulate the behavior of a battery [61–63]. Some other models represent the behavior of a battery using two differential equations. The kinetic battery model (KBM) introduced in [64] is an example of such models which is, in fact, the discrete version of the diffusion model in [65].

Resource allocation and management is another important issue which needs to be taken into account for the design of an energy-efficient MSN, as noted earlier. In [66], optimizing the sensor movement in order to achieve maximum energy efficiency is investigated by introducing a velocity schedule in uniform and non-uniform road conditions. The KBM is used in [67] and a proper energy allocation strategy is utilized for the sensor nodes to address the problem of efficient information routing in wireless sensor networks for maximizing network lifetime. A criterion is developed in [68] to switch between an energy-aware policy and a battery-aware policy in such a way that the lifetime of the network is maximized. An integer nonlinear programming formulation is used in [69] to find the optimal battery allocation for a cost-constrained lifetime maximization problem. A Markov chain model and a simple distributed duty cycle scheme are proposed in [70] to capture the battery recovery effect for increasing the network lifetime.

All of the existing results on lifetime maximization, including the ones cited in this section, consider only one or two of the three major energy consumption sources noted above. This motivates the present work on a comprehensive algorithm which takes into

account all three sources of energy consumption. The main contributions of this thesis and the novel approach used to solve the problem are summarized in the next section.

1.3 Thesis Contributions

In this thesis, the problem of target monitoring in a sensing field with obstacles using an MSN is investigated. It is desired to track a moving target in the field by using a proper strategy governing the communication, sensing and movement of the mobile nodes (as the main sources of energy consumption in the network), in such a way that the lifetime of the network is maximized. The strategy should take into consideration three main constraints: connectivity, obstacle avoidance and collision avoidance. Connectivity means that there is a route from the target to the destination point (where network data is collected and processed) at all times. Obstacle avoidance and collision avoidance, on the other hand, mean that while the sensors move, they do not collide with the obstacles (which are assumed to be fixed) or other sensors in the network. To this end, the field is properly divided into a grid, and a graph is subsequently constructed from this grid, and its edges are properly weighted to reflect the energy consumption in the network. This graph is used to find a “close” estimate of the optimal path for routing information from the target to destination. The graph is then redrawn in such a way that the underlying lifetime maximization problem is translated into the problem of constrained shortest path from the target to destination. This is a well-known routing problem in wireless

sensor networks, for which several algorithms exist in the literature. Furthermore, a proper movement plan for the case when the sensor should be relocated could be very effective in minimizing energy consumption of the sensor.

1.4 Thesis Outline and Publications

The remainder of this thesis is organized as follows. In Chapter 2, the idea behind the conventional Voronoi partitioning is used to define the notion of energy-based Voronoi diagram. A novel network-level algorithm for lifetime maximization is proposed along with several theorems and lemmas to analyze its important properties. Simulations are also provided to demonstrate the effectiveness of the algorithm. Chapter 3 is dedicated to a sensor-level technique to minimize energy consumption due to sensor movement. The proposed method uses a battery model in order to formulate the underlying optimization problem and plan the sensor movement accordingly. Finally, the concluding remarks are summarized in Chapter 4, along with some suggestions for future research directions.

The results of this work have been published in or submitted to the following conferences and journals.

[1] **W. Masoudimansour**, H. Mahboubi, A. G. Aghdam, and K. Sayrafian-Pour, “Maximum Lifetime Strategy for Target Monitoring in Mobile Sensor Networks in Presence of Obstacles,” in *Proceedings of the 51st IEEE Conference on Decision and Control*, 2012 (to appear).

[2] H. Mahboubi, **W. Masoudimansour**, A. G. Aghdam, and K. Sayrafian-Pour, “Maximum Life Span Strategy for Target Tracking in Mobile Sensor Networks,” in *Proceedings of the American Control Conference*, 2011.

[3] H. Mahboubi, **W. Masoudimansour**, A. G. Aghdam, and K. Sayrafian-Pour, “Maximum Lifetime Strategy for Target Monitoring in Mobile Sensor Networks in Presence of Obstacles,” submitted to a journal.

[4] H. Mahboubi, **W. Masoudimansour**, A. G. Aghdam, and K. Sayrafian-Pour, “An Energy-Efficient Target Tracking Strategy for Mobile Sensor Networks,” submitted to a journal.

Chapter 2

Maximum Lifetime Strategy for Target Monitoring in Mobile Sensor Networks in Presence of Obstacles

In this chapter, first, some useful tools which will be used in the design of the main algorithm are provided. To achieve this goal, a variant of the conventional Voronoi diagram has been defined which will take the residual energy of the sensors into account for partitioning the field. Then, a novel method for tracking and monitoring a moving target is presented such that the lifetime of the mobile sensor network is maximized. The main objective is to develop a proper motion strategy for the sensors such that the network lifetime is maximized and, in case of presence of obstacles, they are avoided.

It is assumed that the main sources of energy consumption in the network are sensing, communication, and movement of the sensors. It is also assumed that the obstacles in the field can block communication and sensing capabilities of the sensors. Finally, it is assumed that the field can be represented by a grid of points where sensors and the target can reside on. In the proposed approach, the time is discretized such that in a time instant, the field is partitioned into regions according to the sensors' remaining energy. The grid points are then mapped to the vertices of a graph. Each edge of this graph is properly weighted based on the region where the corresponding vertices belong to. An energy-efficient route is then obtained to transfer information from the target to destination using the shortest path algorithm. The sensors are moved to their new locations and this algorithm is reapplied to the network with the new arrangement of the sensors and the target after a time interval which is preses based on the target's speed. It is shown that under certain conditions the shortest path is a good strategy for the sensors to follow in order to maximize the lifetime of the network.

2.1 Voronoi Partitioning

A Voronoi partitioning is a special partitioning of the space based on the distance of the points of the space to a specific family of objects in that space [71]. This decomposition of the space is widely used in different branches of science, and is highly flexible. Voronoi diagrams and their modified versions are significantly useful as tools for solving a wide

variety of application that contain partitioning of the space as a part of the problem. In the following, the conventional Voronoi diagram and an extended version of it is introduced which is consistent with the objectives of this work.

2.1.1 Conventional Voronoi Diagram

Let \mathbf{S} be a set of n distinct nodes S_1, S_2, \dots, S_n in a 2D space. Partition the space to n convex polygons such that each polygon contains only one node, and that node is the closest node to any point in that polygon among all other nodes. This resulting diagram, which partitions the space, is called Voronoi diagram, and each resulting polygon is called a Voronoi region [72]. The mathematical characterization of each region in the resulting diagram is as follows.

$$\Pi_i = \{Q \in R^2 | d(Q, S_i) \leq d(Q, S_j), \forall j \in \mathbf{n} - \{i\}\} \quad (2.1)$$

where $d(Q, S_i)$ denotes the Euclidean distance between the point Q and node S_i and $\mathbf{n} := \{1, 2, \dots, n\}$. To construct the Voronoi region associated with a node, first the perpendicular bisector of every segment connecting the node to its neighbors is drawn. The smallest polygon created by these perpendicular bisectors which contains the node is the Voronoi region of that node. Fig 2.1 shows a sample of a field containing 10 nodes and their corresponding Voronoi regions.

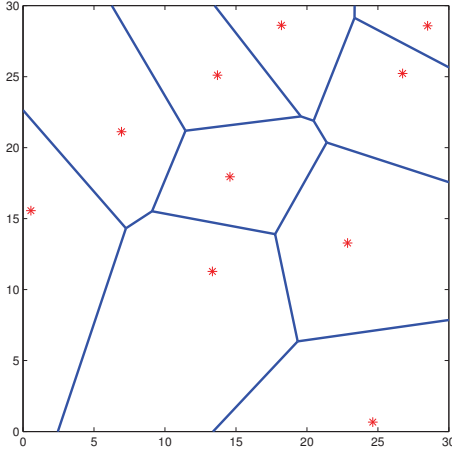


Figure 2.1: An example of a conventional Voronoi partitioning of a field which contains 10 nodes.

2.1.2 Energy-Based Voronoi Diagram

Now, consider a set of n distinct weighted nodes denoted by $\mathbf{S} = \{(S_1, e_1), (S_2, e_2), \dots, (S_n, e_n)\}$,

where $e_i > 0$ is the weighting factor associated with S_i , for any $i \in \mathbf{n} := \{1, 2, \dots, n\}$.

Let the distance between an arbitrary point Q and the weighted node (S_i, e_i) be denoted

by $f(S_i, e_i, Q)$. The *extended Voronoi diagram* is defined as a partitioning of the plane

into n regions with the property that the nearest node (in terms of the distance func-

tion given above) to any point inside a region is the node assigned to that region. The

mathematical characterization of each region obtained by the above partitioning is as

follows:

$$\Pi_i = \{Q \in R^2 | f(S_i, e_i, Q) \leq f(S_j, e_j, Q), \forall j \in \mathbf{n} - \{i\}\} \quad (2.2)$$

Note that for certain functions $f(\cdot)$ and weighting factors e_i , some regions may contain

no points.

Consider now n sensors in a field, and let them be represented by the nodes S_1, S_2, \dots, S_n . The weight of the node S_i in (2.2) is set to be the remaining energy of that sensor. Furthermore, let $f(S_i, e_i, Q)$ be equal to the difference between the initial energy of the i -th sensor, $E_{i,0}$, and the remaining energy of that sensor after traveling to point Q . With no loss of generality, assume that the initial energy of all sensors is the same, and denote it with E_0 . Assume also that the energy required to travel the distance d is linearly proportional to it. Then, one can write:

$$f(S_i, e_i, Q) = (E_{i,0} - e_i) + e_s + \beta d(S_i, Q) \quad (2.3)$$

where β is a known constant, e_s is the energy required to overcome the static friction (when the sensor starts to move) which is assumed to be the same for all sensors. Furthermore, $d(S_i, Q)$ is the shortest distance from S_i to Q (in the sense of the distance function (2.3)). For the particular choice of distance function and weighting factor considered in this work, the extended Voronoi diagram will be referred to as the *energy-based Voronoi (E-Voronoi) diagram* and its characteristics are described in the sequel.

Consider two sensors located at S_1 and S_2 with the remaining energies e_1 and e_2 , respectively. If $f(S_1, e_1, Q) = f(S_2, e_2, Q)$, then:

$$\begin{aligned}
(E_0 - e_1) + e_s + \beta d(S_1, Q) &= (E_0 - e_2) + e_s + \beta d(S_2, Q) \\
\Rightarrow e_1 - e_s - \beta d(S_1, Q) &= e_2 - e_s - \beta d(S_2, Q) \\
\Rightarrow d(S_1, Q) - d(S_2, Q) &= \frac{e_1 - e_2}{\beta} = \text{const.}
\end{aligned} \tag{2.4}$$

Therefore, the loci of every point Q for which $f(S_1, e_1, Q) = f(S_2, e_2, Q)$ is one branch of a hyperbola. In the special case when $e_1 = e_2$, this loci is the perpendicular bisector of the segment S_1S_2 .

To construct the E-Voronoi region associated with a node in the network, first the branches of the above-mentioned hyperbolas of that node and the other nodes are drawn. The smallest region containing each node is, in fact, the region assigned to that node. Fig. 2.2 shows the E-Voronoi diagram for 2 sensors with different amounts of remaining energy.

Now, consider a 2D field with obstacles. When an obstacle is located on the line connecting a sensor to its candidate location, then the sensor cannot move on a straight line, and also its sensing and communication capabilities are attenuated in practice. In particular, in this work it is assumed that the obstacles attenuate the communication and sensing capabilities of the sensors to zero [73]. Fig. 2.3 shows an example of a configuration with a target whose location cannot be detected by the sensor because of

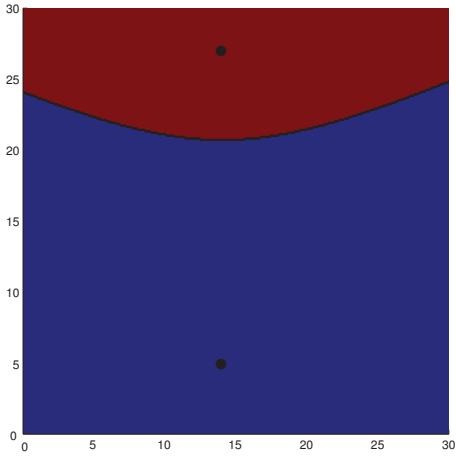


Figure 2.2: An example of the consumed energy Voronoi diagram for 2 sensors with different amounts of remaining energy.

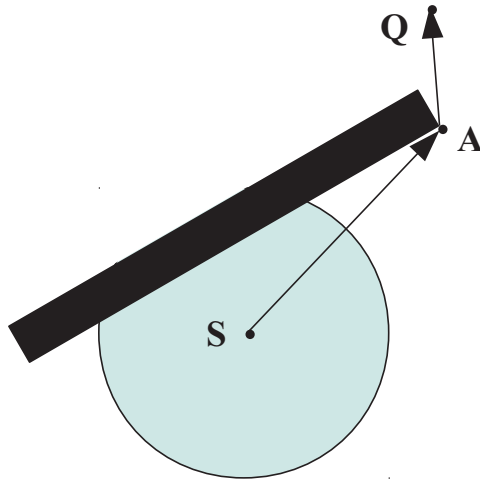


Figure 2.3: An example of a sensor near an obstacle with blocked sensing capability

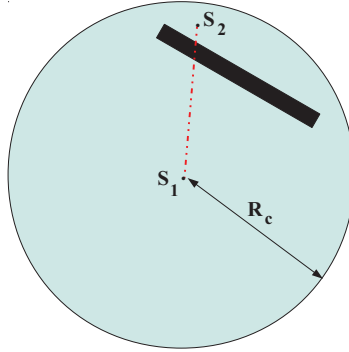


Figure 2.4: An example of a sensor near an obstacle with blocked communication capability

the way the obstacle is positioned. Since the obstacle is blocking the line-of-sight between the points S and Q , the sensor can, for example, move along the segments \overline{SA} , \overline{AQ} which provide the shortest distance in this case. In this work, the shortest distance is used instead of conventional Euclidean distance $d(S, Q)$ to calculate the required movement energy for the sensor in the formulation of the E-Voronoi diagram. Furthermore, as Fig. 2.4 shows, two sensors located on opposite sides of the obstacle cannot communicate even if they are distanced within each others normal communication range. Fig. 2.5 depicts the E-Voronoi diagram in the presence of obstacles for two sensors, which will hereafter be referred to as the *obstructed* energy-based Voronoi (OE-Voronoi) diagram. As it can be observed from this figure, the border lines of an OE-Voronoi diagram in this case are not necessarily branches of hyperbolae, and their shapes are highly dependent on the location of obstacles.

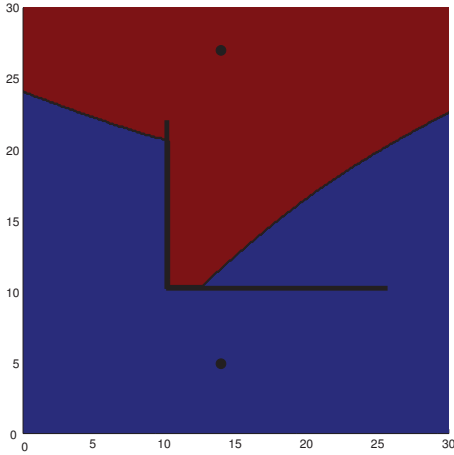


Figure 2.5: An example of the obstructed energy-based Voronoi diagram for two sensors with different levels of remaining energy.

2.2 Problem Formulation

Consider a group of n mobile sensors S_1, \dots, S_n . Consider also a moving target and a fixed access point (also referred to as the destination point). In order to ensure target tracking at all times, it is essential to maintain connectivity (in terms of sensing and communication) between target and destination point.

In order to develop energy-efficient sensor deployment strategies, it is required to adopt a proper model for the energy consumption of sensors. In general, the energy consumption of mobile sensors is mainly due to communication, sensing, and movement. Although minimizing energy consumption is of great importance in MSNs, in many applications it is more desirable that the lifetime of the sensors is maximized, in order to increase the durability of the overall network. An effective strategy to maximize the lifetime of the network is that sensors with small residual energy consume small amounts

of energy such that the residual energy of the sensor with minimum remaining energy among all the sensors is maximized. To this end, sensors must operate in a collaborative fashion in order to determine the best location and routing path for each sensor to transmit the information from target to destination. Since the analytical solution of this problem is complicated in general, as an efficient alternative approach, divide the sensing field into a grid. Assume that the target and sensors are located on some nodes of the grid in each time instant. Then, a graph is constructed whose vertices are the grid nodes, and whose edges are properly weighted, to model the three sources of energy consumption in the network taking lifetime maximization into account. This graph will be referred to as the *energy consumption digraph*. The following notation will prove convenient in the development of the main results.

Notation 2.1. Throughout this chapter, the nearest sensor to node Q in terms of energy consumption, referred to as *EC-nearest* sensor to the node Q , is denoted by S_Q^1 and characterized by:

$$f(S_Q^1, e_{S_Q^1}, Q) \leq f(S_j, e_j, Q), \quad S_Q^1 \in \mathbf{S}, \quad S_j \in \mathbf{S} - \{S_Q^1\} \quad (2.5)$$

where $e_{S_Q^1}$ is the remaining energy of the sensor S_Q^1 . Also, the i -th nearest sensor to node Q (again in terms of energy consumption) is referred to as i -th EC-nearest sensor

to Q , and is denoted by S_Q^i . This can be formulated as:

$$\begin{aligned} f(S_Q^i, e_{S_Q^i}, Q) &\leq f(S_j, e_j, Q), \quad S_Q^i \in \mathbf{S} - \bigcup_{h=1}^{i-1} \{S_Q^h\}, \\ S_j &\in \mathbf{S} - \bigcup_{h=1}^i \{S_Q^h\} \end{aligned} \tag{2.6}$$

where $e_{S_Q^i}$ is the remaining energy of the sensor S_Q^i . Furthermore, $E_{r,Q}^i$ denotes the residual energy of the i -th EC-nearest sensor to Q , after traveling to this point.

Assumption 2.1. It is assumed that the sensor assigned to sense the target in any time instant is the EC-nearest sensor to it, which is hereafter called the *monitoring sensor* at that time instant. Note that this sensor is not necessarily fixed (i.e., it may change from time to time). A subset of other sensors can be employed accordingly to create an information route from target to destination.

Denote the monitoring sensor with S_T (note that $S_T \in \{S_1, S_2, \dots, S_n\}$ at any time instant) and the destination point with P_D . Denote also the target node and the E/OE-Voronoi region containing it with P_T and Π_T , respectively.

Definition 2.1. Any node on the grid which belongs to Π_T and a sensor, if located at that point, can sense the target is hereafter called a *sensing node*. Furthermore, any node of a given path P excluding target and destination is referred to as a *path node* for P .

2.3 Proposed Algorithm

Consider a group of n sensors, and the corresponding OE-Voronoi diagram. Denote the j -th region with Π_j , for any $j \in \mathbf{n}$. A weight-assignment algorithm is provided in the sequel to find candidate locations for the sensors to maximize the network lifetime.

Construct a directed graph (digraph) where an edge from P_T to a node P_j is drawn if and only if P_j is a sensing node. Fig. 2.6 demonstrates the edges originated from P_T for a sample OE-Voronoi diagram. Furthermore, a node P_i ($P_i \neq P_T$) is connected to another node P_j in this digraph if and only if a sensor located at P_i could communicate with a sensor located at P_j . Note that in the case where an obstacle is blocking the line-of-sight between P_i and P_j , there would be no edge between their corresponding vertices in the digraph. The following procedure is used for the weight assignment of the edges in the digraph.

Case 1) Assume P_i and P_j are in different regions OR P_j is the destination node.

Then:

- i) If the target and P_i are in the same region AND P_i is not a sensing node, then the weight of the edge from P_i to P_j is given by:

$$w(i, j) = \left[\frac{E_0 - E_{r, P_i}^2 + \omega_c(P_i, P_j)}{E_0} \right]^k$$

where $\omega_c(P_i, P_j)$ is the communication cost from the node P_i to P_j , and k is a

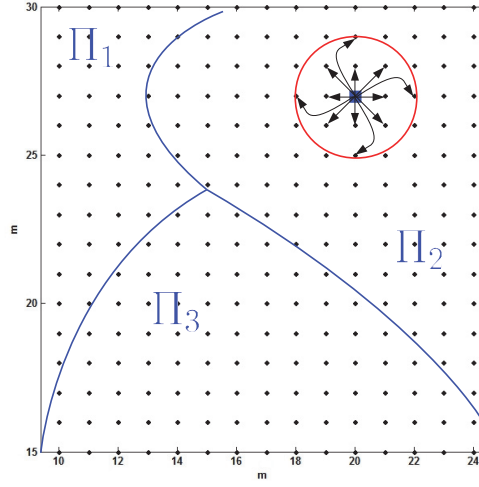


Figure 2.6: Edges originating from the target to the adjacent graph nodes for a sample consumed energy Voronoi diagram.

constant which will be introduced later.

ii) If the target and P_i are in different regions, then:

$$w(i, j) = \left[\frac{E_0 - E_{r, P_i}^1 + \omega_c(P_i, P_j)}{E_0} \right]^k$$

iii) If P_i is a sensing node, then:

$$w(i, j) = \left[\frac{E_0 - E_{r, P_i}^1 + \omega_c(P_i, P_j) + \omega_s(P_T, P_i)}{E_0} \right]^k$$

where $\omega_s(P_T, P_i)$ is the required sensing energy for a sensor at P_i to sense the target.

Case 2) Consider now the case where P_i and P_j are in the same region, AND P_j is not the destination node.

i) If the target and P_i are in the same region AND P_i is not a sensing node, then:

$$w(i, j) = \left[\frac{E_0 - E_{r, P_i}^2 + \omega_c(P_i, P_j)}{E_0} \right]^k$$

ii) If the target and P_i are in different regions, then:

$$w(i, j) = \max \left(\min \left(\left[\frac{E_0 - E_{r, P_i}^1 + \omega_c(P_i, P_j)}{E_0} \right]^k \right. \right. \\ \left. \left. + \left[\frac{E_0 - E_{r, P_j}^2 + \omega_{min}}{E_0} \right]^k, \left[\frac{E_0 - E_{r, P_j}^1 + \omega_c(P_i, P_j)}{E_0} \right]^k \right. \right. \\ \left. \left. + \left[\frac{E_0 - E_{r, P_i}^2 + \omega_{min}}{E_0} \right]^k \right) \right. \\ \left. - \left[\frac{E_0 - E_{r, P_j}^1 + \omega_{max}}{E_0} \right]^k, \left[\frac{E_0 - E_{r, P_i}^1 + \omega_c(P_i, P_j)}{E_0} \right]^k \right)$$

where ω_{min} is the energy required by a sensor on one grid node to communicate with the nearest node to it in the grid, and ω_{max} is the energy required for the communication of two sensors in maximum distance from each other (R_c).

iii) If P_i is a sensing node, then:

$$w(i, j) = \left[\frac{E_0 - E_{r, P_i}^1 + \omega_c(P_i, P_j) + \omega_s(P_T, P_i)}{E_0} \right]^k$$

Fig. 2.7 illustrates sample edges for each of the above cases. In the edge AB , node A is not a sensing node while it is in the same region as the target but it is not in the same region as P_j . Thus, the edge AB is an example of case 1(*i*). On the other hand, CD and EF satisfy the conditions of case 1(*ii*) because EF has vertices in different regions while E is not in the target's region, and D is the destination point. The edge GH represents case 1(*iii*) as G is a sensing node. Moreover, the three edges IJ , KL and MN are examples of cases 2(*i*), 2(*ii*) and 2(*iii*), respectively.

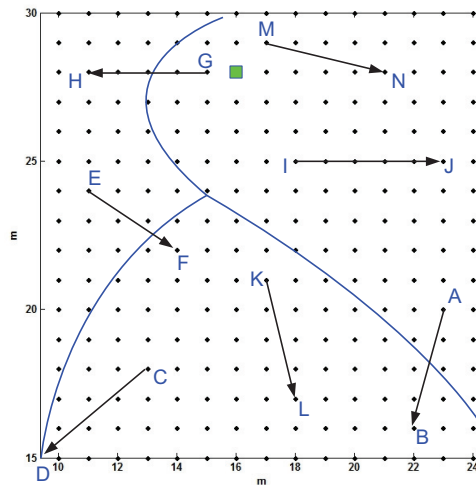


Figure 2.7: Different types of edges for a field with three sensors.

Given an energy consumption digraph, it is desired now to find the shortest path connecting the target to destination, subject to the constraint that the number of nodes in the path is less than or equal to the number of sensors. This path provides an information route which is optimal for lifetime maximization under some conditions as discussed later. Algorithm 1 summarizes the proposed technique.

Algorithm 1

- 1) Divide the field to rectangular grid cells.
 - 2) Partition the field using the extended Voronoi diagram.
 - 3) Construct a digraph with the grid nodes as its vertices.
 - 4) Assign proper weights to the edges of the constructed digraph using the proposed weighting strategy.
 - 5) Find the shortest path connecting the target to the destination point.
 - 6) Move the required sensors to the nodes of the shortest path for establishing the information link.
 - 7) Repeat the algorithm from step 2 after relocating the sensors.
-

Remark 2.1. One can use an efficient routing algorithm (such as Dijkstra) to find the shortest path in the energy consumption digraph. If the number of nodes in the shortest path eventually turns out to be greater than n , then one can switch to a constrained shortest path algorithm, which is typically slower than its unconstrained counterparts.

Definition 2.2. A path P with at most n nodes which connects the target to destination is called a *feasible path*. The sum of the weights of the directed edges of a feasible path P is denoted by $W(P)$; this sum is referred to as the *path weight*.

Definition 2.3. Throughout this chapter, the percentage of the total energy consumption of a sensor is sometimes referred to as the *consumed energy* of that sensor. In other words, consumed energy is equal to the ratio of the difference between the initial energy of a sensor and its residual energy, to its initial energy.

Definition 2.4. Consider a network of n mobile sensors S_1, S_2, \dots, S_n , and a feasible path P with m nodes, denoted by the ordered set $(P_T, P_1, P_2, \dots, P_m, P_D)$. Assume the EC-nearest sensor (among n sensors) to the target is assigned to P_1 . For the rest of the sensors and the path nodes, there are $\binom{n-1}{m-1}$ (combination of $m-1$ out of $n-1$) possible sensor assignments, which together with the sensor assigned to P_1 can be employed to transfer the information from P_T to P_D in this case. Let the assignment of the distinct sensors $S_{i_1}, S_{i_2}, \dots, S_{i_m}$ to the nodes P_1, P_2, \dots, P_m , respectively, be denoted by the pair (P, S_P) , where S_P represents the ordered set $(S_{i_1}, S_{i_2}, \dots, S_{i_m})$. Furthermore, denote with (P, S_P^*) the sensor assignment for which the energy consumption of the sensor with the smallest residual energy (after relocating the sensors and transmitting information from target to destination) is minimum, and call it the *optimal assignment*. It is important to note that the optimal sensor assignment can change each time the sensors are relocated. However, to simplify notation, the time-dependence has not been explicitly shown in the above representation.

Definition 2.5. Consider the optimal assignment (P, S_P^*) for a mobile sensor network. The k -th power of the consumed energy of the sensor S_{i_j} after traveling to node P_j and collaborating in information transmission will be referred to as *node cost* of P_j in path P and will hereafter be denoted by $C_P(P_j)$. Furthermore, the sum of node costs of all the path nodes of P will be called *path cost* of P and will be denoted by $C(P)$.

Theorem 2.1. *For any feasible path P in an energy consumption digraph, the relation*

$W(P) \leq C(P)$ holds.

Proof. Assume the feasible path $P = (P_T, P_1, P_2, \dots, P_m, P_D)$ passes through regions $\Pi_1, \Pi_2, \dots, \Pi_m$, and the path has n_i nodes in region Π_i , $i = 1, 2, \dots, m$. Partition P into h sub-paths as follows:

$$P^1 = (P_T, P_1^1, P_2^1, \dots, P_{n_1}^1, P_1^2)$$

$$P^2 = (P_1^2, P_2^2, \dots, P_{n_2}^2, P_1^3)$$

\vdots

$$P^m = (P_1^h, P_2^h, \dots, P_{n_m}^h, P_D)$$

Now, it suffices to show that for any sub-path, the path weight is less than or equal to the corresponding path cost. If Π_a contains exactly one node for any $a = 1, 2, \dots, m$, then the sub-path P^a contains only the edge (P_1^a, P_1^{a+1}) (note that P_1^{m+1} is, in fact, P_D). The weight assigned to this edge in the digraph is $\left[\frac{E_0 - E_{r, P_1^a}^1 + \omega_c(P_1^a, P_1^{a+1})}{E_0} \right]^k$ for $a \neq 1$ and $\left[\frac{E_0 - E_{r, P_1^a}^1 + \omega_c(P_1^a, P_1^{a+1}) + \omega_s(P_T, P_1^a)}{E_0} \right]^k$ for $a = 1$, which correspond to the assignment of the EC-nearest sensor to the node P_1^a . It is important to note that in both cases the assigned weight is equal to the minimum combined cost of movement, communication, and sensing of a sensor after moving to P_1^a . If the EC-nearest sensor to P_1^a is also the EC-nearest sensor to some other nodes in the path, the weight is less than the cost.

On the other hand, if Π_a contains more than one node, there will be two possibilities as follows:

Case 1: $a \neq 1$. In this case, every edge from P_i to P_j has either the weight

$$\min \left(\left[\frac{E_0 - E_{r,P_i}^1 + \omega_c(i,j)}{E_0} \right]^k + \left[\frac{E_0 - E_{r,P_j}^2 + \omega_{min}}{E_0} \right]^k, \left[\frac{E_0 - E_{r,P_j}^1 + \omega_c(i,j)}{E_0} \right]^k + \left[\frac{E_0 - E_{r,P_i}^2 + \omega_{min}}{E_0} \right]^k \right) - \left[\frac{E_0 - E_{r,P_j}^1 + \omega_{max}}{E_0} \right]^k$$

or

$$\left[\frac{E_0 - E_{r,P_i}^1 + \omega_c(i,j)}{E_0} \right]^k$$

Let the former be called *type A* edge and the latter *type B* edge. Now, divide the sub-path P^a to l sub²-paths as follows:

$$P^{a,1} = P_1^{a,1}, P_2^{a,1}, \dots, P_{m_1}^{a,1}, P_1^{a,2}$$

$$P^{a,2} = P_1^{a,2}, P_2^{a,2}, \dots, P_{m_2}^{a,2}, P_1^{a,3}$$

\vdots

$$P^{a,l} = P_1^{a,l}, P_2^{a,l}, \dots, P_{m_l}^{a,l}, P_1^{a+1,1}$$

such that the last edge in any sub-path $P^{a,b}$, $b = 1, 2, \dots, l$ is a type B edge, and the rest of the edges in that sub-path are of type A. Obviously in any region Π_a there is at least one sub-path, and every sub-path contains at least one type B edge.

Assume now that the EC-nearest sensor to all nodes of Π_a is assigned to one of the nodes of a sub²-path $P^{a,b}$, $1 \leq b \leq l$ of the sub²-paths of P^a . In this case, the weight assigned to the sub-path $P^{a,b}$ is:

$$W^b(a) = \sum_{q=1}^{m_b-1} \left[\min \left(g(1, P_q^{a,b}, P_{q+1}^{a,b}) + g_{\min}(2, P_{q+1}^{a,b}), g(1, P_{q+1}^{a,b}, P_q^{a,b}) + g_{\min}(2, P_q^{a,b}) \right) - g_{\max}(1, P_{q+1}^{a,b}) \right] + g(1, P_{m_b}^{a,b}, P_1^{a,b+1}) \quad (2.7)$$

where $g(u, P_i, P_j) = \left[\frac{E_0 - E_{r, P_i}^u + \omega_c(P_i, P_j)}{E_0} \right]^k$, $g_{\min}(u, P_i) = \left[\frac{E_0 - E_{r, P_i}^u + \omega_{\min}}{E_0} \right]^k$ and $g_{\max}(u, P_i) = \left[\frac{E_0 - E_{r, P_i}^u + \omega_{\max}}{E_0} \right]^k$. From the properties of the OE-Voronoi diagram, the EC-nearest sensor to all nodes of the sub-path $P^{a,b}$ is the same, but it can move to only one node. Thus, the cost of moving m_b sensors to m_b nodes of the sub-path, which will be denoted by $C^b(a)$ satisfies the following relation:

$$C^b(a) \geq g(1, P_j^{a,b}, P_{j+1}^{a,b}) + \sum_{q=1, q \neq j}^{m_b} g(2, P_q^{a,b}, P_{q+1}^{a,b}), \quad (2.8)$$

$$\forall j \in \{1, 2, \dots, m_b\}$$

It is now straightforward to derive the following relations:

$$\begin{aligned} W_{a,1}^b &= \sum_{q=1}^{j-1} g(1, P_{q+1}^{a,b}, P_{q+2}^{a,b}) + g_{\min}(2, P_q^{a,b}) - g(1, P_{q+1}^{a,b}, P_{q+2}^{a,b}) \\ &\geq \sum_{q=1}^{j-1} \min \left(g(1, P_q^{a,b}, P_{q+1}^{a,b}) + g_{\min}(2, P_{q+1}^{a,b}), g(1, P_{q+1}^{a,b}, P_{q+2}^{a,b}) + g_{\min}(2, P_q^{a,b}) \right) \\ &\quad - g(1, P_{q+1}^{a,b}, P_{q+2}^{a,b}) \end{aligned} \quad (2.9)$$

$$\begin{aligned}
W_{a,2}^b &= \left[\sum_{q=j}^{m_b-1} g(1, P_q^{a,b}, P_{q+1}^{a,b}) + g_{\min}(2, P_{q+1}^{a,b}) - g(1, P_{q+1}^{a,b}, P_{q+2}^{a,b}) \right] + g(1, P_{m_b}^{a,b}, P_1^{a,b+1}) \\
&\geq \left[\sum_{q=j}^{m_b-1} \min \left(g(1, P_q^{a,b}, P_{q+1}^{a,b}) + g_{\min}(2, P_{q+1}^{a,b}), g(1, P_{q+1}^{a,b}, P_{q+2}^{a,b}) + g_{\min}(2, P_q^{a,b}) \right) \right. \\
&\quad \left. - g(1, P_{q+1}^{a,b}, P_{q+2}^{a,b}) \right] + g(1, P_{m_b}^{a,b}, P_1^{a,b+1})
\end{aligned} \tag{2.10}$$

By expanding the right side of the above relations and simplifying them, it is concluded that:

$$\begin{aligned}
W_{a,1}^b + W_{a,2}^b &= g(1, P_j^{a,b}, P_{j+1}^{a,b}) + \sum_{q=1, q \neq j}^{m_b} g(2, P_q^{a,b}, P_{q+1}^{a,b}) \\
&\geq \sum_{q=1}^{m_b-1} \left[\min \left(g(1, P_q^{a,b}, P_{q+1}^{a,b}) + g_{\min}(2, P_{q+1}^{a,b}), g(1, P_{q+1}^{a,b}, P_{q+2}^{a,b}) + g_{\min}(2, P_q^{a,b}) \right) \right. \\
&\quad \left. - g(1, P_{q+1}^{a,b}, P_{q+2}^{a,b}) \right] + g(1, P_{m_b}^{a,b}, P_1^{a,b+1})
\end{aligned} \tag{2.11}$$

Since $g(u, P_i, P_j) \leq g_{\max}(u, P_i)$ for any integer u and any points P_i and P_j , the following relation is obtained:

$$\begin{aligned}
&\sum_{q=1}^{m_b-1} \left[\min \left(g(1, P_q^{a,b}, P_{q+1}^{a,b}) + g_{\min}(2, P_{q+1}^{a,b}), g(1, P_{q+1}^{a,b}, P_{q+2}^{a,b}) + g_{\min}(2, P_q^{a,b}) \right) \right. \\
&\quad \left. - g(1, P_{q+1}^{a,b}, P_{q+2}^{a,b}) \right] + g(1, P_{m_b}^{a,b}, P_1^{a,b+1}) \geq \sum_{q=1}^{m_b-1} \left[\min \left(g(1, P_q^{a,b}, P_{q+1}^{a,b}) \right. \right. \\
&\quad \left. \left. + g_{\min}(2, P_{q+1}^{a,b}), g(1, P_{q+1}^{a,b}, P_{q+2}^{a,b}) + g_{\min}(2, P_q^{a,b}) \right) - g_{\max}(1, P_{q+1}^{a,b}) \right] + g(1, P_{m_b}^{a,b}, P_1^{a,b+1}) \\
&= W^b(a)
\end{aligned} \tag{2.12}$$

Finally, from (2.8), (2.11) and (2.12), one arrives at:

$$C^b(a) \geq W^b(a)$$

Now, for the other sub-paths $P^{a,c}$, $c = 1, 2, \dots, l$, $c \neq b$, one can write:

$$\begin{aligned} C^c(a) &\geq \sum_{q=1}^{m_c} g(2, P_q^{a,c}, P_{q+1}^{a,c}) \\ &\geq g(1, P_j^{a,c}, P_{j+1}^{a,c}) + \sum_{q=1, q \neq j}^{m_c} g(2, P_q^{a,c}, P_{q+1}^{a,c}), \quad \forall j; j \in \{1, 2, \dots, m_c\} \end{aligned}$$

Using a similar approach:

$$C^c(a) \geq W^c(a)$$

Note that the weight and cost of the sub-path in region Π_a are the sum of the weights and costs of its sub²-paths of that region. Thus, for region Π_a :

$$C(a) \geq W(a), \quad a = 2, 3, \dots, m$$

Case 2: $a = 1$ (the region contains the target). In this case, the EC-nearest sensor to the nodes of this region is assigned to detect the target, and hence, cannot be assigned to another node. Thus, the cost of the sub-path P^1 satisfies the following relation:

$$C(1) \geq g_s(1, P_1^1, P_2^1) + \sum_{q=2}^{n_1} g(2, P_q^1, P_{q+1}^1)$$

where, $g_s(u, P_i, P_j) = \left[\frac{E_0 - E_{r, P_i}^u + \omega_c(P_i, P_j) + \omega_s(P_T, P_i)}{E_0} \right]^k$. On the other hand, the proposed

weight-assignment strategy yields:

$$W(1) = g_s(1, P_1^1, P_2^1) + \sum_{q=2}^{n_1} g(2, P_q^1, P_{q+1}^1)$$

and hence:

$$C(1) \geq W(1)$$

This completes the proof. □

Definition 2.6. A *good path* is defined as a feasible path P with the following properties:

- i) It has at most two nodes in the region Π_T and at most one node in other regions.
- ii) If the region Π_T contains exactly two nodes of the path, say P_i and P_j , creating a directed edge from P_i to P_j , then the path P does not pass through the region containing the second EC-nearest sensor to P_j . Moreover, a feasible path P with at most one node in each OE-Voronoi region is referred to as a *perfect path*. It is obvious that any perfect path is a good path as well.

Definition 2.7. Consider a network of n mobile sensors and a feasible path P with m nodes, and let the optimal assignment (P, S_p^*) be deployed. Let also the maximum energy consumption (from the initial time of the network operation) amongst all sensors once they move to their assigned nodes and transmit information from target to destination be referred to as the *max-min energy consumption* w.r.t. the path P , and denoted by

$E(P, S_P^*)$.

Definition 2.8. Among all feasible paths, the one w.r.t. which the max-min energy consumption is minimum will be referred to as the *optimal path*, and denoted by P^* .

Theorem 2.2. *For any feasible good path, the path weight and path cost are equal.*

Proof. Consider the following two cases:

Case 1: Region Π^a , $a = 1, 2, \dots, n$ contains only one node. In this case, it is important to note that in the optimal assignment of a good path, the EC-nearest sensor is assigned to node P_i in region Π^a . On the other hand, the proposed weight-assignment strategy assigns the weight $g(1, P_i, P_{i+1})$ to the edge $P_i P_{i+1}$. Thus, the path cost and path weight for the edge in region Π^a are equal.

Case 2: Region Π^T contains the sensing node P_i as well as the node P_{i+1} . In this case, since the EC-nearest sensor is assigned to sense the target, the optimal assignment will be that of the EC-nearest sensor to P_i and the second EC-nearest sensor to P_{i+1} . Note that, from definition of a good path, the second EC-nearest sensor to P_{i+1} is not assigned to any other node. Moreover, the weights of the edges $P_i P_{i+1}$ and $P_{i+1} P_{i+2}$ are $g_s(1, P_i, P_{i+1})$ and $g(2, P_{i+1}, P_{i+2})$, respectively. Therefore, the path cost and path weight are equal for this case as well.

From the above discussion (which is valid for any region), it is concluded that the path cost and path weight of a feasible good path are equal. □

Remark 2.2. Since any perfect path is also a good path, the result of Theorem 2.2 holds for any feasible perfect path as well.

Definition 2.9. A feasible path P is said to be θ -optimal if the difference between $E(P, S_P^*)$ and $E(P^*, S_{P^*}^*)$ is at most equal to θ , i.e, $E(P, S_P^*) - E(P^*, S_{P^*}^*) \leq \theta$.

Lemma 2.1. For any positive real numbers n, x, θ , where $x, \theta \leq 1$, if $k > \frac{\ln(n)}{\ln(1+\theta)}$ then

$$(x + \theta)^k > nx^k$$

Proof. The inequality $k > \frac{\ln(n)}{\ln(1+\theta)}$ yields

$$(1 + \theta)^k > n \tag{2.13}$$

Since $x \leq 1$, thus

$$\left(1 + \frac{\theta}{x}\right)^k \geq (1 + \theta)^k \tag{2.14}$$

It results from (2.13) and (2.14) that $(1 + \frac{\theta}{x})^k > n$, or equivalently $(x + \theta)^k > nx^k$. \square

Theorem 2.3. Apply the proposed weight-assignment strategy to an arbitrary constant $k > \frac{\ln(n)}{\ln(1+\theta)}$. If the shortest path \bar{P} in the energy consumption digraph is a good path, then it is θ -optimal.

Proof. Consider the shortest path \bar{P} with the corresponding optimal assignment, and let the sensor that consumes the minimum energy $E(\bar{P}, S_{\bar{P}}^*)$ be denoted by \bar{S}_1 . The

following two cases are investigated:

Case 1: \bar{S}_1 is not assigned to any node of \bar{P} . Consider the optimal path P^* and the corresponding optimal assignment $S_{P^*}^*$. If \bar{S}_1 is not assigned to any node of the optimal path P^* either, then $E(P^*, S_{P^*}^*) = E(\bar{P}, S_{\bar{P}}^*)$. If, on the other hand, \bar{S}_1 is assigned to one of the nodes of the optimal path, then its energy consumption is greater than $E(\bar{P}, S_{\bar{P}}^*)$. Note that the energy consumption of \bar{S}_1 is less than or equal to $E(P^*, S_{P^*}^*)$, which implies that $E(\bar{P}, S_{\bar{P}}^*) \leq E(P^*, S_{P^*}^*)$. By definition, this means that \bar{P} is the optimal path. The proof is complete now on noting that any optimal path is θ -optimal as well.

Case 2: \bar{S}_1 is assigned to a node of \bar{P} . In this case, if \bar{P} is not a θ -optimal path, then:

$$\begin{aligned} E(\bar{P}, S_{\bar{P}}^*) &> E(P^*, S_{P^*}^*) + \theta \Rightarrow \\ [E(\bar{P}, S_{\bar{P}}^*)]^k &> [E(P^*, S_{P^*}^*) + \theta]^k \end{aligned} \tag{2.15}$$

Also, according to Lemma 2.1:

$$[E(P^*, S_{P^*}^*) + \theta]^k \geq n [E(P^*, S_{P^*}^*)]^k \tag{2.16}$$

From the definition of path cost and max-min energy consumption and on noting that

there are at most n sensors in any feasible path, it results that:

$$C(\bar{P}) \geq [E(\bar{P}, S_{\bar{P}}^*)]^k \quad (2.17)$$

$$n [E(P^*, S_{P^*}^*)]^k \geq C(P^*) \quad (2.18)$$

Relations (2.15), (2.16), (2.17) and (2.18) yield:

$$C(\bar{P}) > C(P^*) \quad (2.19)$$

On the other hand, from Theorem 2.1:

$$C(P^*) \geq W(P^*) \quad (2.20)$$

Also, since \bar{P} is a good path, according to Theorem 2.2:

$$C(\bar{P}) = W(\bar{P}) \quad (2.21)$$

From (2.19), (2.20) and (2.21), it is concluded that $W(\bar{P}) > W(P^*)$, which is in contradiction with the fact that \bar{P} is the shortest path. Therefore, \bar{P} is a θ -optimal path. \square

Corollary 2.1. *Choose $k > \frac{\ln(n)}{\ln(1+\theta)}$; if the shortest path \bar{P} is a perfect path, then it is θ -optimal too.*

Proof. The proof follows immediately Theorem 2.3 and on noting that any perfect path is a good path as well. □

2.4 Simulation Results

Consider 20 identical sensors which are randomly deployed in a field of size $30\text{m} \times 30\text{m}$. A target is moving in the field, and the sensors are to track it and route its information to the destination point which is assumed to be in the origin. Suppose all sensors have communication and sensing ranges of 10m and 3m, respectively. Communication and sensing energies are assumed to be $\omega_c(P_i, P_j) = \mu[d(P_i, P_j)]^\lambda$ and $\omega_s(P_T, P_j) = \zeta[d(P_T, P_j)]^\gamma$, respectively, where $d(P_i, P_j)$ is the Euclidean distance between the points P_i and P_j , as noted before. It is also assumed that the required energy for a sensor to travel from a point P_i to another point P_j is equal to $\beta d(P_i, P_j)$ where $d(P_i, P_j)$ is the smallest distance the sensor has to move to reach P_j from P_i . It is important to note that in case of the presence of obstacles, $d(P_i, P_j)$ is not necessarily simply the euclidean distance. In addition, θ is considered to be 0.15 which yields $k > 21.43$.

The following values are used for system parameters in the simulations: $\mu = 10^{-3}$, $\zeta = 10^{-3}$, $\beta = 7.54$, $\lambda = 2$ and $\gamma = 2$. It is also assumed that the target moves based on a Markov movement in random integer steps in the interval $[-1, 1]$ along both horizontal and vertical axes. The field is divided to a grid of size 30×30 . The algorithm determines the route and the new candidate locations for the sensors in discrete time instants. The

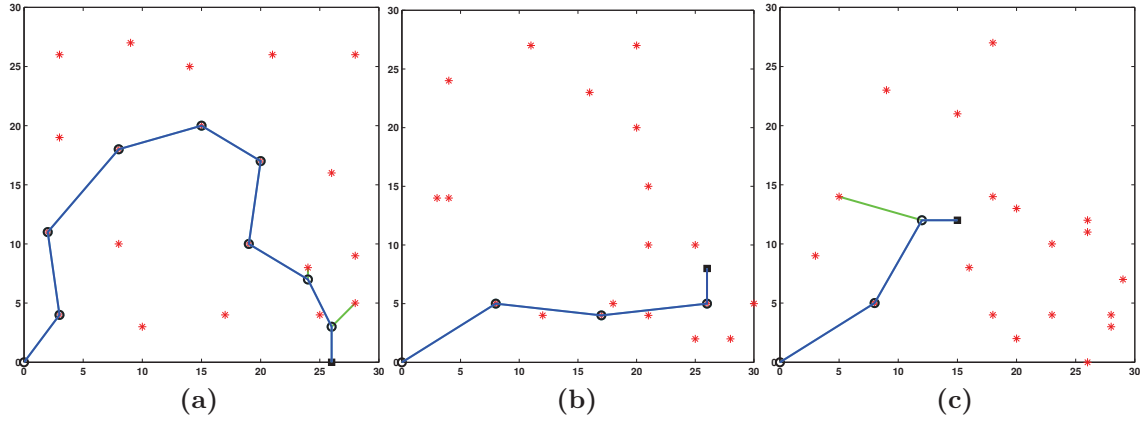


Figure 2.8: Snapshots of the network utilizing the proposed technique for 20 sensors in three different iterations.

time interval between these instants is chosen based on the target's speed. Simulation is performed for two scenarios.

Definition 2.10. Network lifetime is defined as the time in which the first sensor among all the sensors depletes its energy completely. There are different definitions for network lifetime in the literature, however, this definition is used widely ([24], [25], [26]), and it is used in this work as well.

Scenario 1:

In this case there are no obstacles in the field. Fig. 2.8 demonstrates the route and the candidate locations of the sensors for three different time instants. In each step, the location of the target and sensors as well as the shortest path in the constructed energy consumption digraph are depicted. The current location of the sensors are shown by asterisks, while their calculated candidate locations to move to are depicted by small

circles. The location of the target is shown by a square, and the shortest path is shown by blue segments. Furthermore, green lines show the movement of the sensors from their current locations to the candidate points in case they need to move. Note that under the proposed algorithm, nearest sensors to the path nodes in the sense of Euclidean distance are not necessarily assigned to them (see Fig. 2.8(a),(c)). Also, it can be seen in the figure that, sometimes, the algorithm may choose a communication route that is longer than other possible routes, however, this is due to the fact that the algorithm tries to make use of the sensors which have more residual energy.

Remark 2.3. Simulation results show that for different network setups with different number of sensors and specification, in most of the cases the shortest path in the proposed algorithm is either a good path or a perfect path, which according to Theorem 2.3 is θ -optimal as well.

To prove the effectiveness of the proposed technique, it must be compared with a similar algorithm for tracking and monitoring which takes all major sources of energy depletion into account. In [1], such a comprehensive algorithm is proposed which considers movement, communication and sensing as the most important energy consuming factors for minimizing the overall energy consumption of a sensor network. This algorithm is applied to the above setup, and the result is compared with the proposed technique. As Fig. 2.9 illustrates, the proposed algorithm outperforms the algorithm in [1], where the former keeps the network alive for 459 iterations and the latter keeps it alive for 1450

iterations. Also, one can observe that since in the proposed algorithm, a sensor with more energy is more likely to take part in transmitting the information, the energies of all the sensors are very close to each other during depletion. This means that the algorithm uses the energy from all the sensors. This result is, indeed, expected since in the former algorithm, the residual energy of the sensors is not an effective parameter in making the decision for the information route. Moreover, the tracking sensor in the former algorithm can be a specific sensor for many iterations, especially when the target is moving slowly. While in our proposed technique, the sensing sensor changes in case a sensor depletes large amount of energy for tracking the target.

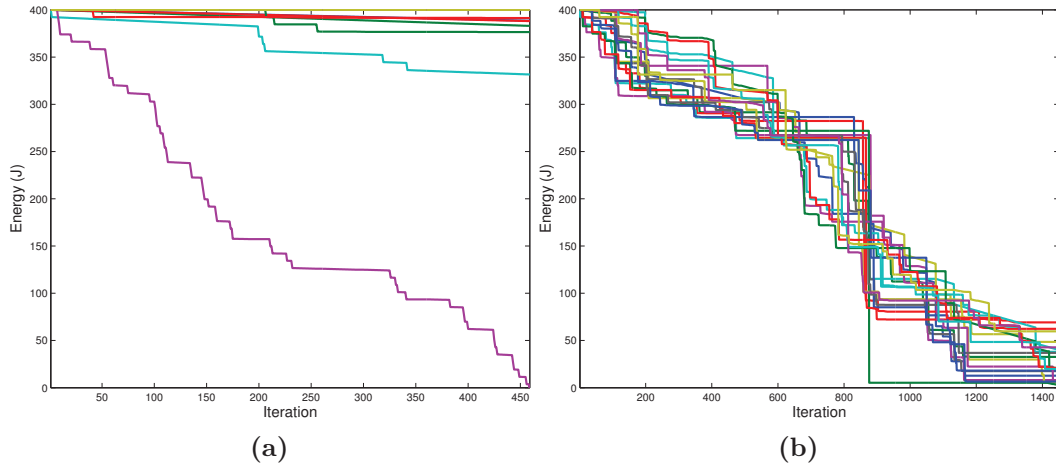


Figure 2.9: Energy of the sensors during network lifetime: (a) tracking algorithm from [1]; (b) proposed algorithm.

Scenario 2:

In the second scenario, the above mentioned field is used for simulation while two solid obstacles are considered to be in the field. The chosen route and sensors

for information transmission are shown in Fig. 2.10 for three different snapshots of the network.

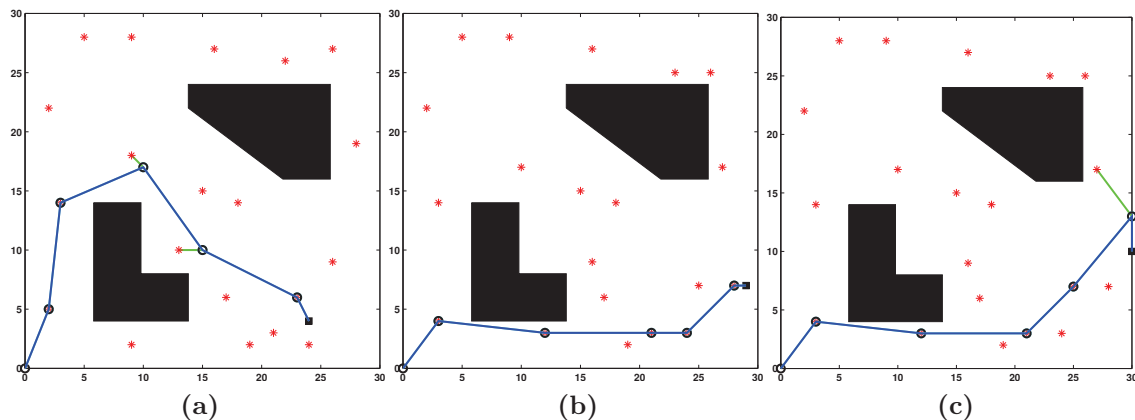


Figure 2.10: Snapshots of the network configuration obtained by the proposed technique for 20 sensors in three different steps.

To assess the performance of the proposed technique in presence of obstacles, it will be compared to the algorithm developed in [74] for minimizing the overall energy consumption of a sensor network. Fig. 2.11 (a) depicts the remaining energy of sensors v.s. iteration number under the algorithm given in [1], while Fig. 2.11 (b) provides analogous results using the proposed algorithm. These figures show that utilizing the algorithm introduced in this work the lifetime of the network increases by 69%. They also show that the consumption of energy in different nodes is more balanced under the proposed algorithm, which further demonstrates the efficiency of the method.

Remark 2.4. It is important to note that if the target is moving smoothly in the field, then under the technique proposed in [1] the tracking sensor does not change frequently,

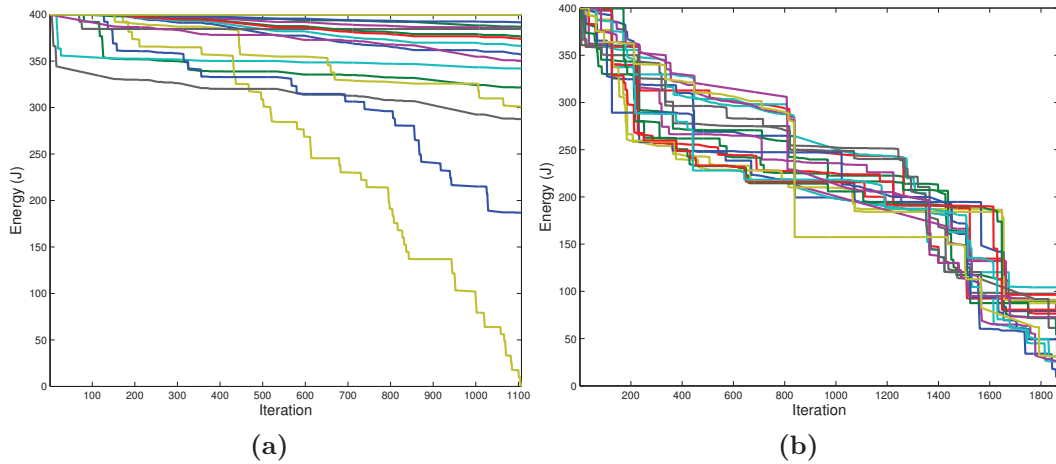


Figure 2.11: Energy of the sensors during network lifetime in presence of obstacles: (a) tracking algorithm from [1]; (b) proposed algorithm.

as it continues to be the nearest sensor to the target. As a result, the energy of the tracking sensor in [1] is depleted fast. However, since in the method proposed here, the EC-nearest sensor to the target is defined based on the residual energy of the sensors, the tracking sensor can be changed appropriately. This prevents each sensor from quickly depleting its energy.

2.5 Summary

In this chapter, an extension of the conventional Voronoi diagram is presented which proves useful in designing the proposed technique. This extended Voronoi diagram is based on the residual energy of the sensors which makes it a useful tool for partitioning the field based on the general idea of reducing energy consumption of the sensors with

small residual energy. Then, a novel technique was proposed in this chapter to prolong the lifetime of a mobile sensor network that is monitoring a moving target in a field with potential obstacles. Energy consumption of the network is mainly due to sensing, communication, and movement of the sensors. A digraph is constructed by transforming the field to a grid and using the grid nodes as vertices. As the main contribution of this work, the edges of the digraph are weighted with respect to the remaining energy of the sensors. Using this digraph, the lifetime maximization problem can be transformed into a shortest path problem. Detailed simulations demonstrate the effectiveness of the proposed strategy in finding best relocation pattern for the mobile sensors, as well as the best route to transfer the target information.

Chapter 3

Movement Planning with Respect to Battery Model for Lifetime Optimization in Mobile Sensor Networks

In this chapter, an efficient energy management and movement planning technique is proposed. It is assumed that the dominant source of energy consumption in the sensor is movement. The proposed method exploits both battery characteristics and mobile sensor's actuator energy consumption properties to find the optimal movement plan. The KBM model is used for the battery, and the mobile sensor is assumed to be actuated

using DC micro-motors. Using the energy dynamics of the battery and the practical constraints on the velocities, accelerations, time and distance, the network lifetime maximization is formulated as a nonlinear programming problem whose solution provides the optimal movement plan for the sensor. The planned movement, then, can be used in case a sensor needs to change location based on the proposed algorithm from the previous chapter.

3.1 Problem Statement

Let the battery power consumption be modeled as two interconnected wells representing two sources of energy as shown in Fig. 3.1. This model is called *kinetic battery model* (KBM) [64], and the two sources of energy are called *available charge* (A-well) and *bound charge* (B-well). As it can be seen from the figure, the content of the A-well is directly available to the load. The B-well energy, on the other hand, is available indirectly through its interconnection to the A-well. This model takes two significant effects into account: (i) The heavier the load on a battery, the shorter its lifetime. This effect is known as rate capacity effect, and means that by taking higher current from the battery until it is dead, higher portion of its energy (corresponding to the B-well) will remain unused. (ii) Another important fact about this model is the recovery effect. The battery can replenish itself to some degree when it is not being used (through the interconnection between two wells, hence flow of energy from the B-well to A-well). This

recovery process can prolong the lifetime of the mobile sensor.

The energy of a mobile sensor is depleted in different ways. Major sources of energy consumption in mobile sensors are movement, communication and sensing. However, energy consumption due to movement dominates the other two. Therefore, a proper moving strategy for the sensors can play an important role in improving network lifetime. Assume that a mobile sensor is required to move a certain distance within a limited time. According to the KBM, it may be desirable that the sensor stops once or more to replenish itself before reaching its destination so that the energy of the B-well transfers to the A-well. To this end, one can divide the sensor travel time interval to a number of sub-intervals for the sensors to move and stop over two consecutive sub-intervals. The sub-intervals can be obtained by introducing a proper objective function for energy consumption, and solving the corresponding optimization problem. In practice, one should take the limitations on sensor acceleration/deceleration and velocity into consideration, which leads to a constrained optimization problem. The mechanical characteristics of the motor also needs to be incorporated in the energy consumption model.

3.2 Proposed Strategy

Consider a DC-motor-powered sensor connected to a battery, and let the two-well model described in the previous section be used to represent the battery. Let the available

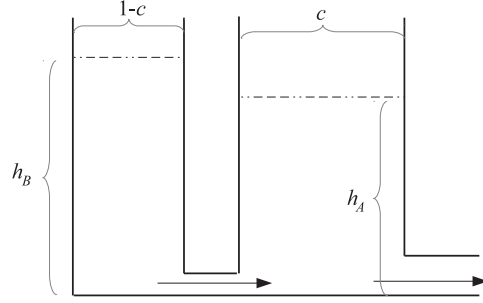


Figure 3.1: The two-well battery model

charge well and the bound charge well energy content in the KBM be represented by E_A and E_B , respectively. Also, denote the total energy capacity of the battery by E_T . Initially, it is assumed that, the two wells are in equilibrium (with the same height), and that their contents are $E_A(0) = cE_T$ and $E_B(0) = (1 - c)E_T$, where c is a constant coefficient which depends on the battery specifications. The interconnection between the two wells in Fig. 3.1 is represented by the conductance k , which controls the energy flow rate from the B-well to A-well. The flow rate also depends on the height difference between the two wells. Denote the heights of the A and B-wells at time t by $h_A(t) = \frac{E_A(t)}{c}$ and $h_B(t) = \frac{E_B(t)}{(1-c)}$. The following differential equations describe the energy flow dynamics of the battery [64]:

$$\begin{aligned} \frac{dE_A(t)}{dt} &= -P(t) + k \left[\frac{E_B(t)}{(1-c)} - \frac{E_A(t)}{c} \right] \\ \frac{dE_B(t)}{dt} &= -k \left[\frac{E_B(t)}{(1-c)} - \frac{E_A(t)}{c} \right] \end{aligned} \tag{3.1}$$

with the initial conditions:

$$E_A(0) = cE_T$$

$$E_B(0) = (1 - c)E_T$$

where $P(t)$ is the power delivered to the load. A battery is said to be dead when the charge in the A-well reaches zero, i.e. $E_A(t) = 0$.

Mobile sensors are typically powered by electromechanical motors. DC micro-motors, for instance, are the most commonly used actuators. The voltage of the armature of a DC motor obeys the following equation:

$$V(t) = R_a I(t) + K_e \omega(t) \quad (3.2)$$

where R_a and $I(\cdot)$ represent the armature resistance and current, respectively. Also, K_e is the back electromotive force (emf) coefficient, and $\omega(t)$ is the angular velocity of the rotor. In addition, it is known that:

$$I(t) = \frac{1}{K_T} \left[J \frac{d\omega(t)}{dt} + T_L + D\omega(t) \right] \quad (3.3)$$

where K_T is a constant coefficient relating the torque to armature current. Also, J is the combined inertia of the rotor and the load, and T_L is the resistive torque of the load. The coefficient D is the viscose damping parameter, which also generates a resistive

torque for the motor.

The power $P(t)$ delivered to the load is an implicit function of the motor parameters, acceleration and velocity. The differential equations (3.1) can be solved in closed form over each sub-interval described in the previous section. In a movement sub-interval the sensor is assumed to accelerate to the velocity v for time t_a , move with constant velocity v for time t_c , and decelerate to velocity 0 for time t_d . Let the solutions to (3.1) be represented by:

$$\begin{aligned} E_A(t_a + t_c + t_d) &= f_A(t_a, t_c, t_d, v, E_{A,0}, E_{B,0}) \\ E_B(t_a + t_c + t_d) &= f_B(t_a, t_c, t_d, v, E_{A,0}, E_{B,0}) \end{aligned} \tag{3.4}$$

where $E_{A,0}$ and $E_{B,0}$ are the contents of the A and B-wells at the beginning of the movement period, respectively. Similarly, when the sensor stops for a sub-interval of length t_r and hence the battery is not used in this period, let the solutions to (3.1) be represented by:

$$\begin{aligned} E_A(t_r) &= g_A(t_r, E_{A,0}, E_{B,0}) \\ E_B(t_r) &= g_B(t_r, E_{A,0}, E_{B,0}) \end{aligned} \tag{3.5}$$

Now, consider a mobile sensor moving on wheels powered by a DC motor, and

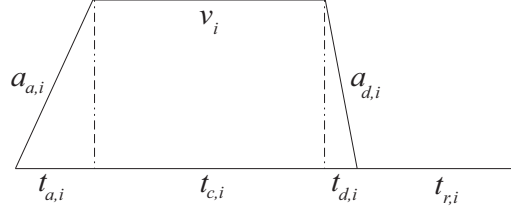


Figure 3.2: A sample movement/replenishing period in a planned sensor movement.

assume that this sensor is to move the distance L in a limited time T . Assume also that the sensor stops n times as it moves to the target location. As discussed earlier, the sensor accelerates for time $t_{a,1}$ with a constant acceleration $a_{a,1}$. Then it moves with a constant velocity v_1 for time $t_{c,1}$, and finally it decelerates to zero velocity for time $t_{d,1}$ with a constant deceleration $a_{d,1}$. The total moving time will hereafter be called *movement period*. The sensor stops for time $t_{r,1}$, referred to as *replenishing period*. This sequence of movement/replenishing periods is repeated n times until the sensor reaches its destination.

The accelerations in the above-mentioned movement periods will be denoted by $a_{a,1}, a_{a,2}, \dots, a_{a,n}$, with the corresponding times $t_{a,1}, t_{a,2}, \dots, t_{a,n}$. Also, the decelerations in the movement periods will be denoted by $a_{d,1}, a_{d,2}, \dots, a_{d,n}$, with the corresponding times $t_{d,1}, t_{d,2}, \dots, t_{d,n}$. Furthermore, the constant (non-zero) velocity times are represented by $t_{c,1}, t_{c,2}, \dots, t_{c,n}$, with the corresponding velocities v_1, v_2, \dots, v_n , and the replenishing time intervals are denoted by $t_{r,1}, t_{r,2}, \dots, t_{r,n}$. These parameters are shown for a sample movement period and the subsequent replenishing period in Fig. 3.2.

As the sensor moves, the energy contents of the two wells evolve by time as described by (3.1). Let the energy contents of the A-well and B-well at the end of each movement be denoted by $E_{Am,i}$ and $E_{Bm,i}$, respectively, for $i = 1, 2, \dots, n$. Denote also, the energy of the A-well and B-well at the end of a replenishing period by $E_{Ar,i}$ and $E_{Br,i}$, respectively.

Definition 3.1. The energy difference between the A-well and B-well after the sensor moves to its desired location will be referred to as *unavailable energy*.

Definition 3.2. In this chapter, the total energy consumption of the motor in the time interval $[0, \tau]$ is represented by:

$$G(\tau) = \int_0^{\tau} P(t) dt$$

It is important to note that the unavailable energy results from the difference between the heights of the energy wells A and B. On the other hand, according to (3.1), when the two wells' energy contents are balanced, the maximum possible energy is available in the A-well to be provided to the load. Thus, it is desirable to keep the difference between the heights of the two energy wells as small as possible for efficient resource management. Furthermore, it is desired to minimize the energy consumption of the motor in order to prolong the battery lifetime. To this end, the following nonlinear programming problem is introduced:

$$\text{minimize: } \lambda_1 G(T) + \lambda_2 \left(\frac{E_{Br,n}}{(1-c)} - \frac{E_{Ar,n}}{c} \right) \quad (3.6a)$$

s.t.

$$t_{a,i}, t_{c,i}, t_{d,i}, t_{r,i} \geq 0, \quad i = 1, 2, \dots, n \quad (3.6b)$$

$$0 \leq v_i \leq v_{max} \quad (3.6c)$$

$$|a_{a,i}|, |a_{d,i}| \leq a_{max} \quad (3.6d)$$

$$E_{Am,i}, E_{Bm,i}, E_{Ar,i}, E_{Br,i} \geq 0 \quad (3.6e)$$

$$E_{Ar,n} \geq \epsilon \quad (3.6f)$$

$$\sum_{j=1}^n (t_{a,j} + t_{c,j} + t_{d,j} + t_{r,j}) = T \quad (3.6g)$$

$$a_{a,i} = \frac{v_i}{t_{a,i}}, \quad a_{d,i} = -\frac{v_i}{t_{d,i}} \quad (3.6h)$$

$$\sum_{j=1}^n v_j t_{c,j} + \frac{1}{2} \sum_{j=1}^n v_j (t_{a,j} + t_{d,j}) = L \quad (3.6i)$$

$$\begin{aligned}
E_{Am,i} &= f_A(t_{a,i}, t_{c,i}, t_{d,i}, v_i, E_{Ar,(i-1)}, E_{Br,(i-1)}) \\
E_{Bm,i} &= f_B(t_{a,i}, t_{c,i}, t_{d,i}, v_i, E_{Ar,(i-1)}, E_{Br,(i-1)}) \\
E_{Ar,i} &= g_A(t_{r,i}, E_{Am,i}, E_{Bm,i}) \\
E_{Br,i} &= g_B(t_{r,i}, E_{Am,i}, E_{Bm,i})
\end{aligned} \tag{3.6j}$$

where a_{max} and v_{max} denote the maximum acceleration and velocity of the sensors. The objective function (3.6a) is introduced to address the above-mentioned desired properties for the motion plan, i.e. minimizing the energy consumption and maximizing the immediate available energy. The weighting parameters λ_1 and λ_2 are constant numbers which are chosen properly to specify the relative importance of energy consumption vs. immediate availability of energy.

In addition to the difference between the heights of the two energy wells, the final energy of the A-well is important as it is the energy available to the load in the next move. This condition is given by the relation (3.6f), where ϵ is a proper constant. The constrained optimization is, in fact, a nonlinear programming problem, which can be solved numerically for any given n , using existing techniques such as gradient-based and interior-point methods [75]. This results in the optimal velocity profile and the corresponding times.

Remark 3.1. It is worth mentioning that n can also be considered as a variable in the above problem, in which case it is transformed to a mixed integer programming which

is highly complex.

3.3 Simulation Results

In this section, the proposed motion planning technique is utilized to improve the lifetime of the sensor battery. Consider a sensor powered by DC micro-motors, and assume that it is to move a distance L in time T . Let the numerical values of the motor parameters be $R_a = 22$, $K_e = 6.5 \times 10^{-3}$, $K_T = 6.6 \times 10^{-3}$, $J = 1.08 \times 10^{-7}$, $T_L = 1.1 \times 10^{-3}$ and $D = 2 \times 10^{-6}$. Let also the maximum velocity and acceleration that can be provided by the motor for the motion of the sensor be $1.2 \frac{\text{m}}{\text{s}}$ and $6.4 \frac{\text{m}}{\text{s}^2}$, respectively. Moreover, assume that the sensor battery parameters be $c = 0.625$, $k = 4.5 \times 10^{-5}$. Note that these parameters can be obtained by experiments.

Using the above setup, the efficiency of the proposed technique is demonstrated in two examples.

Example 1: In this example, the mobile sensor is required to move 800m in 5000s. Choose $\lambda_1 = 10^2$, $\lambda_2 = 1$ and $\epsilon = 0$, and assume the total energy of the battery is $E_T = 8.64 \times 10^4 \text{J}$. Fig. 3.3 shows the movement profile for $n = 2$. As expected, the battery is replenished while the sensor does not move. Solving the resultant nonlinear programming problem, the optimal values $t_a = [10, 7.088] \text{s}$, $t_c = [2366, 129] \text{s}$, $t_d = [0.048, 0.082] \text{s}$, $t_r = [2028, 460] \text{s}$, $a_a = [38.5, 92.3] \frac{\text{m}}{\text{s}^2}$ and $a_d = [-8000, -8000] \frac{\text{m}}{\text{s}^2}$ are obtained. Fig. 3.4 provides the energy profile of the sensor movement. As it can

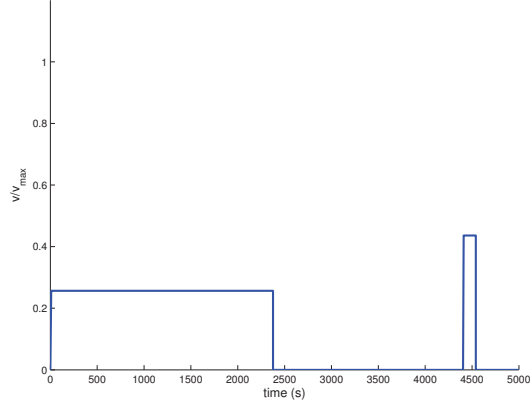


Figure 3.3: Movement profile of sensor in Example 1 for $n = 2$.

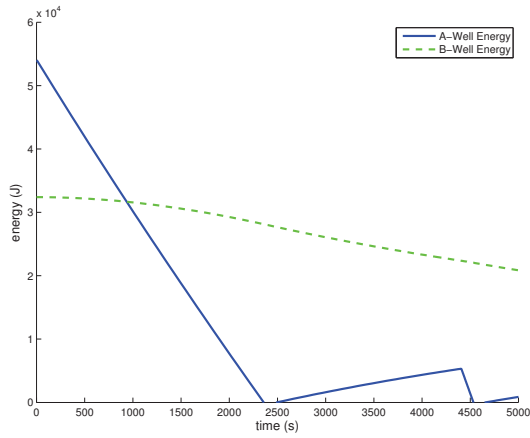


Figure 3.4: Energy profile of sensor in Example 1 for $n = 2$.

be observed from the figure, part of the lost energy of the A-well is recovered in the replenishing period.

Examlpe 2: In this example, the effectiveness of the proposed technique in improving the lifetime of the mobile sensor is investigated. In this example, it is assumed that a mobile sensor is deployed for target tracking (see e.g. [1], [76]). The distance L is a uniformly distributed random value in the interval $[0, 100]$ m, and $T = 600$ s. Also, the parameters of the battery are $c = 0.625$, $k = 4.5 \times 10^{-5}$ and $E_T = 6.912 \times 10^5$.

To prove the effectiveness of the proposed motion planning algorithm, it is compared with a simple motion pattern where the sensor travels distance L with a constant speed of $\frac{L}{T}$. The results are depicted in Figs. 3.5 and 3.6, which demonstrate significant improvement in the battery lifetime using the method presented in this work. The blue and green curves in these figures provide the energies of the A-well and B-well, respectively. This shows that under the proposed technique, a good portion of consumed energy is provided by the B-well, which is not directly available to the load.

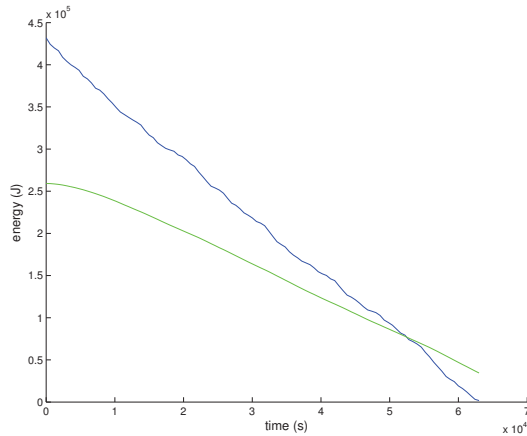


Figure 3.5: Energy profile of the sensor without movement planning in Example 2.

3.4 Summary

An efficient sensor motion planning algorithm utilizing characteristics of the sensor battery has been proposed in this chapter. The algorithm is the solution to a nonlinear optimization problem that is formulated by using an appropriate battery model. The strategy assumes that each sensor moves a predetermined distance in a limited time,

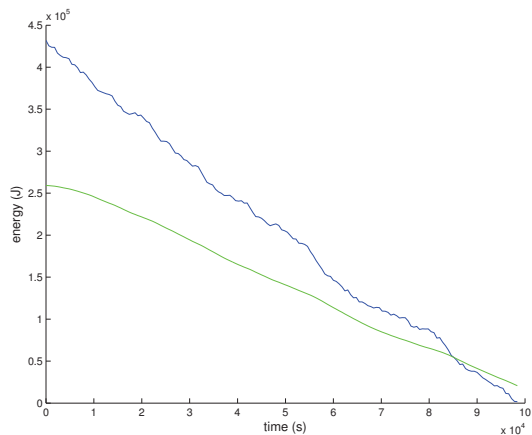


Figure 3.6: Energy profile of the sensor with movement planning in Example 2.

and the movement pattern consists of a sequence of motion-rest periods. Simulation results indicate the effectiveness of the proposed algorithm in prolonging the lifetime of the network. If the mobile sensors have energy harvesting capabilities, the proposed technique can be easily extended to accommodate the harvested energy in addition to the limited battery power.

Chapter 4

Conclusions and Future Work

4.1 Conclusions

The problem of lifetime maximization in a target-tracking mobile sensor network (MSN) in the presence of fixed obstacles was studied in this work. It was assumed that the target moves randomly in the field, and that a link is required to exist at all times from the target to destination node, where network data is collected and processed. First, the energy-based Voronoi diagram was defined based on the residual energy of the sensors, and using the idea behind the conventional Voronoi partitioning. The field was then divided into a grid and mapped into a graph with the grid nodes as its vertices. It was assumed also that the sensors and the target could only reside on the grid nodes. Note that this is a realistic assumption for the case when the size of the

grid cells is sufficiently small compared to that of the Voronoi regions. Proper weights were subsequently assigned to the edges of the graph based on the three dominant sources of energy consumption: communication, sensing and movement. The problem of finding a desirable route and selecting proper locations for the sensors in order to achieve an energy-efficient tracking was translated into the well-known shortest path problem. It was shown that under certain conditions the resulting shortest path is a “close” approximation of the optimal path which maximizes the network lifetime. The efficacy of the developed results were verified by simulation.

It follows from the definition of network lifetime that minimizing the energy consumption of individual sensors has a direct impact on the durability of the network. Taking the characteristics of the battery and motor (the latter being the actuator moving the sensor) into consideration, a strategy was developed in this work to minimize the energy consumption of each sensor (note that typically energy consumption due to sensor movement is much more than that due to communication and sensing). Using proper models for the battery and motor, the problem was formulated as a nonlinear optimization problem and solved subsequently to obtain the desired velocity profile for each sensor.

4.2 Suggestions for Future Work

The present work provides a framework for further analysis of lifetime in an MSN, and development of efficient strategies to address the problem. Given the flexibility and scalability of the proposed techniques, one can use more accurate models for battery and motor to obtain more effective strategies. The impact of obstacles on the communication and sensing capabilities of each sensor would also be an important direction for future research, because the resultant distortions in communication and sensing can have a negative impact on the performance of any lifetime maximizing strategy. Moreover, in some applications the obstacles are not fixed. Extending the results of this thesis to the case of moving obstacles would be very important in such applications.

The presented work provides a framework for further investigation of lifetime in MSNs. Flexibility, scalability, and comprehensiveness of the proposed technique in terms of taking all major energy consumption sources into account facilitates its utilization for improving the lifetime in wide variety of MSNs. However, as few simplifying assumptions regarding the communication of each sensor and the impact of obstacles on this coverage were made, the efficiency of the proposed technique needs to be further investigated with practical implementation of this algorithm. The effect of obstacles on communication and sensing signal attenuation can be investigated more thoroughly. Also, adaptive sensing and communication range for each sensor with regard to its remaining energy is a significant step to prolong the network lifetime which is considered as a future work,

and eventually, energy harvesting techniques (e.g. solar cells) can be exploited in mobile sensors which their effect on optimal velocity profile must be studied carefully.

Bibliography

- [1] H. Mahboubi, W. Masoudimansour, A. G. Aghdam, and K. Sayrafian-Pour, “Cost-efficient routing with controlled node mobility in sensor networks,” in *Proceedings of the IEEE Multi-Conference on Systems and Control*, pp. 1238–1243, 2011.
- [2] S. Ferrari, R. Fierro, and D. Tolic, “A geometric optimization approach to tracking maneuvering targets using a heterogeneous mobile sensor network,” in *Proceedings of the Joint 48th IEEE Conference on Decision and Control and 28th Chinese Control Conference*, pp. 1080–1087, 2009.
- [3] H. M. La and W. Sheng, “Moving targets tracking and observing in a distributed mobile sensor network,” in *Proceedings of the American Control Conference*, pp. 3319–3324, 2009.
- [4] H. M. La, T. H. Nguyen, C. H. Nguyen, and H. N. Nguyen, “Optimal flocking control for a mobile sensor network based a moving target tracking,” in *Proceedings of the*

- IEEE International Conference on Systems, Man and Cybernetics*, pp. 4801–4806, 2009.
- [5] X. Chen, H. Bai, L. Xia, and Y. C. Ho, “Design of a randomly distributed sensor network for target detection,” *Automatica*, vol. 43, pp. 1713–1722, 2007.
- [6] X. Wang, J. Ma, S. Wang, and D. Bi, “Distributed energy optimization for target tracking in wireless sensor networks,” *IEEE Transactions on Mobile Computing*, vol. 9, no. 1, pp. 73–86, 2010.
- [7] F. Agyei-Ntim and K. Newman, “Lifetime estimation of wireless body area sensor network for patient health monitoring,” in *Proceedings of the 31st Annual International Conference of the IEEE Engineering in Medicine and Biology Society: Engineering the Future of Biomedicine*, pp. 1659–1662, 2009.
- [8] S. Saadaoui and L. Wolf, “Architecture concept of a wireless body area sensor network for health monitoring of elderly people,” in *Proceedings of the 4th Annual IEEE Consumer Communications and Networking Conference*, pp. 722–726, 2007.
- [9] A. Milenkovic, C. Otto, and E. Jovanov, “Wireless sensor networks for personal health monitoring: issues and an implementation,” *Computer Communications*, vol. 29, no. 13-14, pp. 2521–2533, 2006.

- [10] Y. He, W. Zhu, and L. Guan, "Optimal resource allocation for pervasive health monitoring systems with body sensor networks," *IEEE Transactions on Mobile Computing*, vol. 10, no. 11, pp. 1558–1575, 2011.
- [11] C. Thomas and N. Balakrishnan, "Improvement in intrusion detection with advances in sensor fusion," *IEEE Transactions on Information Forensics and Security*, vol. 4, no. 3, pp. 542–551, 2009.
- [12] A. Olteanu, Y. Xiao, K. Wu, and X. Du, "An optimal sensor network for intrusion detection," in *Proceedings of the IEEE International Conference on Communications*, pp. 1–5, 2009.
- [13] S. Shin, T. Kwon, G. Y. Jo, Y. Park, and H. Rhy, "An experimental study of hierarchical intrusion detection for wireless industrial sensor networks," *IEEE Transactions on Industrial Informatics*, vol. 6, no. 4, pp. 744–757, 2010.
- [14] P. K. Biswas and S. Phoha, "A sensor network test-bed for an integrated target surveillance experiment," in *Proceedings of the 29th Annual IEEE International Conference on Local Computer Networks*, pp. 552–553, 2004.
- [15] H. C. Lin, Y. C. Kan, and Y. M. Hong, "The comprehensive gateway model for diverse environmental monitoring upon wireless sensor network," *IEEE Sensors Journal*, vol. 11, no. 5, pp. 1293–1303, 2011.

- [16] K. Chintalapudi, T. Fu, J. Paek, N. Kothari, S. Rangwala, J. Caffrey, R. Govindan, E. Johnson, and S. Masri, “Monitoring civil structures with a wireless sensor network,” *IEEE Internet Computing*, vol. 10, no. 2, pp. 26–34, 2006.
- [17] Y. Tselishchev and A. Boulis, “Wireless sensor network tested for structural health monitoring of bridges,” in *Proceedings of the IEEE Sensors Conference*, pp. 1796–1799, 2009.
- [18] B. Chen and W. Liu, “Mobile agent computing paradigm for building a flexible structural health monitoring sensor network,” *Computer-Aided Civil and Infrastructure Engineering*, vol. 25, no. 7, pp. 504–516, 2010.
- [19] H. C. Lin, Y. C. Kan, and Y. M. Hong, “The comprehensive gateway model for diverse environmental monitoring upon wireless sensor network,” *IEEE Sensors Journal*, vol. 11, no. 5, pp. 1293–1303, 2011.
- [20] M. Shuai, K. Xie, X. Ma, and G. Song, “An on-road wireless sensor network approach for urban traffic state monitoring,” in *Proceedings of the 11th International IEEE Conference on Intelligent Transportation Systems*, pp. 1195–1200, 2008.
- [21] B. Barbagli, I. M. G. Manes, A. Manes, G. Langer, and M. Bacchi, “A distributed sensor network for real-time acoustic traffic monitoring and early queue detection,” in *Proceedings of the 4th International Conference on Sensor Technologies and Applications*, pp. 173–178, 2010.

- [22] J. H. Chang and L. Tassiulas, “Maximum lifetime routing in wireless sensor networks,” *IEEE/ACM Transactions on Networking*, vol. 12, no. 4, pp. 609–619, 2004.
- [23] X. Wu and G. Chen, “Dual-sink: using mobile and static sinks for lifetime improvement in wireless sensor networks,” in *Proceedings of the 16th International Conference on Computer Communications and Networks*, pp. 1309–1314, 2007.
- [24] J. Park and S. Sahni, “An online heuristic for maximum lifetime routing in wireless sensor networks,” *IEEE Transactions on Computers*, vol. 55, pp. 1048–1056, 2006.
- [25] J. Kim, X. Lin, N. B. Shroff, and P. Sinha, “On maximizing the lifetime of delay-sensitive wireless sensor networks with anycast,” in *Proceedings of the IEEE INFOCOM*, pp. 1481–1489, 2008.
- [26] C. C. Hung, K. C. J. Lin, C. C. Hsu, C. F. Chou, and C. J. Tu, “On enhancing network-lifetime using opportunistic routing in wireless sensor networks,” in *Proceedings of the International Conference on Computer Communications and Networks*, pp. 1–6, 2010.
- [27] W. Wang, V. Srinivasan, and K. C. Chua, “Using mobile relays to prolong the lifetime of wireless sensor networks,” in *Proceedings of the Annual International Conference on Mobile Computing and Networking*, pp. 270–283, 2005.
- [28] I. Dietrich and F. Dressler, “On the lifetime of wireless sensor networks,” *ACM Transactions on Sensor Networks*, vol. 5, no. 1, 2009.

- [29] W. Liang, J. Luo, and X. Xu, "Prolonging network lifetime via a controlled mobile sink in wireless sensor networks," in *Proceedings of the IEEE Global Communications Conference*, pp. 1–6, 2010.
- [30] M. Gatzianas and L. Georgiadis, "A distributed algorithm for maximum lifetime routing in sensor networks with mobile sink," *IEEE Transactions on Wireless Communications*, vol. 7, no. 3, pp. 984–994, 2008.
- [31] H. Kim, T. Kwon, and P. Mah, "Multiple sink positioning and routing to maximize the lifetime of sensor networks," *IEICE Transactions on Communications*, vol. E91-B, no. 11, pp. 3499–3506, 2008.
- [32] S. Shen, A. Zhan, P. Yang, and G. Chen, "Exploiting sink mobility to maximize lifetime in 3d underwater sensor networks," in *Proceedings of the IEEE International Conference on Communications*, pp. 1–5, 2010.
- [33] J. Luo and J. P. Hubaux, "Joint sink mobility and routing to maximize the lifetime of wireless sensor networks: The case of constrained mobility," *IEEE/ACM Transactions on Networking*, vol. 18, no. 3, pp. 871–884, 2010.
- [34] X. Xu and W. Liang, "Placing optimal number of sinks in sensor networks for network lifetime maximization," in *Proceedings of the IEEE International Conference on Communications*, pp. 1–6, 2011.

- [35] H. Yuan, J. Xie, and N. Hu, "Lifetime-optimal sensor deployment for wireless sensor networks with mobile sink," in *Proceedings of the 6th IEEE Joint International Information Technology and Artificial Intelligence Conference*, vol. 1, pp. 451–454, 2011.
- [36] Z. Cheng, M. Perillo, and W. B. Heinzelman, "General network lifetime and cost models for evaluating sensor network deployment strategies," *IEEE Transactions on Mobile Computing*, vol. 7, no. 4, pp. 484–497, 2008.
- [37] D. Wang, B. Xie, and D. P. Agrawal, "Coverage and lifetime optimization of wireless sensor networks with gaussian distribution," *IEEE Transactions on Mobile Computing*, vol. 7, no. 12, pp. 1444–1458, 2008.
- [38] Y. Chen, T. Ren, Z. Wang, and Y. Ping, "Lifetime maximization routing based on genetic algorithm for wireless sensor networks," *Advanced Materials Research*, vol. 230-232, pp. 283–287, 2011.
- [39] C. C. Lai, C. K. Ting, and R. S. Ko, "An effective genetic algorithm to improve wireless sensor network lifetime for large-scale surveillance applications," in *Proceedings of the IEEE Congress on Evolutionary Computation*, pp. 3531–3538, 2007.
- [40] X. M. Hu, J. Zhang, Y. Yu, H. S. H. Chung, Y. L. Li, Y. H. Shi, and X. N. Luo, "Hybrid genetic algorithm using a forward encoding scheme for lifetime maximization of wireless sensor networks," *IEEE Transactions on Evolutionary Computation*,

vol. 14, no. 5, pp. 766–781, 2010.

- [41] D. B. Jourdan and O. L. de Weck, “Layout optimization for a wireless sensor network using a multi-objective genetic algorithm,” in *Proceedings of the 59th IEEE Vehicular Technology Conference*, vol. 5, pp. 2466–2470, 2004.
- [42] C. C. Liao and C. K. Ting, “Extending wireless sensor network lifetime through order-based genetic algorithm,” in *Proceedings of the IEEE International Conference on Systems, Man and Cybernetics*, pp. 1434–1439, 2008.
- [43] Z. Zeshun, L. Layuan, X. Yi, and W. Xiangli, “An efficient energy routing algorithm based on dynamic programming in wireless sensor networks,” in *Proceedings of the 5th International Conference on Wireless Communications, Networking and Mobile Computing*, pp. 1–4, 2009.
- [44] M. U. Ilyas and H. Radha, “A dynamic programming approach to maximizing a statistical measure of the lifetime of sensor networks,” *ACM Transactions on Sensor Networks*, vol. 8, no. 2, 2012.
- [45] J. L. Williams, J. W. Fisher, and A. S. Willsky, “An approximate dynamic programming approach for communication constrained inference,” in *Proceedings of the 13th IEEE Workshop on Statistical Signal Processing*, pp. 1129–1134, 2005.

- [46] J. L. Williams and J. W. Fisher, "Approximate dynamic programming for communication-constrained sensor network management," *IEEE Transactions on Signal Processing*, vol. 55, no. 8, pp. 4300–4311, 2007.
- [47] M. Cordina and C. J. Debono, "Increasing wireless sensor network lifetime through the application of some neural networks," in *Proceedings of the 3rd International Symposium on Communications, Control, and Signal Processing*, pp. 467–471, 2008.
- [48] Y. Shen and B. Guo, "Dynamic power management based on wavelet neural network in wireless sensor networks," in *Proceedings of IFIP International Conference on Network and Parallel Computer Workshops*, pp. 431–436, 2007.
- [49] R. Machado and S. Tekinay, "Neural network-based approach for adaptive density control and reliability in wireless sensor networks," in *Proceedings of the IEEE Wireless Communications and Networking Conference*, pp. 2537–2542, 2008.
- [50] M. Cordina and C. J. Debono, "Maximizing the lifetime of wireless sensor networks through intelligent clustering and data reduction techniques," in *Proceedings of the IEEE Wireless Communications and Networking Conference*, pp. 1–6, 2009.
- [51] M. Hasegawa, T. Kawamura, H. N. Tran, G. Miyamoto, Y. Murata, H. Harada, and S. Kato, "Decentralized optimization of wireless sensor network lifetime based on neural network dynamics," in *Proceedings of the 19th IEEE International Symposium on Personal, Indoor and Mobile Radio Communications*, pp. 1–5, 2008.

- [52] S. Yu and C. S. G. Lee, “Mobility and routing joint design for lifetime maximization in mobile sensor networks,” in *Proceedings of the IEEE/RSJ International Conference on Intelligent Robots and Systems*, pp. 2300–2305, 2011.
- [53] S. Yu and C. S. G. Lee, “Lifetime maximization in mobile sensor networks with energy harvesting,” in *Proceedings of the IEEE International Conference on Robotics and Automation*, pp. 5911–5916, 2011.
- [54] J. Zhu, J. Cao, M. Liu, Y. Zheng, H. Gong, and G. Chen, “A mobility prediction-based adaptive data gathering protocol for delay tolerant mobile sensor network,” in *Proceedings of the IEEE Global Telecommunications Conference*, pp. 1–5, 2008.
- [55] L. Karim and N. Nasser, “Energy efficient and fault tolerant routing protocol for mobile sensor network,” in *Proceedings of the IEEE International Conference on Communications*, pp. 1–5, 2011.
- [56] M. Rahimi, H. Shah, G. S. Sukhatme, J. Heideman, and D. Estrin, “Studying the feasibility of energy harvesting in a mobile sensor network,” in *Proceedings of the IEEE International Conference on Robotics and Automation*, vol. 1, pp. 19–24, 2003.
- [57] M. Doyle, T. F. Fuller, and J. Newman, “Modeling of galvanostatic charge and discharge of the lithium/polymer/insertion cell,” *Journal of the Electrochemical Society*, vol. 140, no. 6, pp. 1526–1533, 1993.

- [58] T. F. Fuller, M. Doyle, and J. Newman, "Simulation and optimization of the dual lithium ion insertion cell," *Journal of the Electrochemical Society*, vol. 141, no. 1, pp. 1–10, 1994.
- [59] E. D. Gadjeva and I. H. Partenov, "Behavioral spice models of lithium ion batteries in the charge stage," in *Proceedings of the 13th International Scientific and Applied Science Conference*, pp. 82–87, 2005.
- [60] S. Gold, "A pspice macromodel for lithium-ion batteries," in *Proceedings of the 12th Annual Battery Conference on Applications and Advances*, pp. 215–222, 1997.
- [61] C. F. Chiasserini and R. R. Rao, "Improving battery performance by using traffic shaping techniques," *IEEE Journal on Selected Areas in Communications*, vol. 19, no. 7, pp. 1385–1394, 2001.
- [62] C. F. Chiasserini and R. R. Rao, "Energy efficient battery management," *IEEE Journal on Selected Areas in Communications*, vol. 19, no. 7, pp. 1235–1245, 2001.
- [63] C. F. Chiasserini and R. R. Rao, "A model for battery pulsed discharge with recovery effect," in *Proceedings of the IEEE Wireless Communications and Networking Conference*, vol. 2, pp. 636–639, 1999.
- [64] J. F. Manwell and J. G. McGowan, "Lead acid battery storage model for hybrid energy systems," *Solar Energy*, vol. 50, no. 5, pp. 399–405, 1993.

- [65] D. N. Rakhmatov and S. B. K. Vrudhula, “An analytical high-level battery model for use in energy management of portable electronic systems,” in *Proceedings of the IEEE/ACM International Conference on Computer Aided Design*, pp. 488–493, 2001.
- [66] G. Wang, M. J. Irwin, H. Fu, P. Berman, W. Zhang, and T. L. Porta, “Optimizing sensor movement planning for energy efficiency,” *ACM Transactions on Sensor Networks*, vol. 7, no. 4, 2011.
- [67] X. Ning and C. G. Cassandras, “On maximum lifetime routing in wireless sensor networks,” in *Proceedings of the Joint 48th IEEE Conference on Decision and Control and 28th Chinese Control Conference*, pp. 3757–3762, 2009.
- [68] R. Rao, S. Vrudhula, and N. Chang, “Battery optimization vs energy optimization: Which to choose and when?,” in *Proceedings of the IEEE/ACM International Conference on Computer-Aided Design*, vol. 2005, pp. 438–444, 2005.
- [69] H. Long, Y. Liu, Y. Wang, R. P. Dick, and H. Yang, “Battery allocation for wireless sensor network lifetime maximization under cost constraints,” in *Proceedings of the IEEE/ACM International Conference on Computer-Aided Design*, pp. 705–712, 2009.

- [70] C. K. Chau, F. Qin, S. Sayed, M. H. Wahab, and Y. Yang, “Harnessing battery recovery effect in wireless sensor networks: Experiments and analysis,” *IEEE Journal on Selected Areas in Communications*, vol. 28, no. 7, pp. 1222–1232, 2010.
- [71] A. Okabe, *Spatial tessellations: concepts and applications of Voronoi diagrams*. Wiley series in probability and statistics: Applied probability and statistics, Wiley, 2000.
- [72] R. Klein, *Concrete and Abstract Voronoi Diagrams*. Lecture Notes in Computer Science, Springer, 1989.
- [73] Y. C. Wang, C. C. Hu, and Y. C. Tseng, “Efficient deployment algorithms for ensuring coverage and connectivity of wireless sensor networks,” in *Proceedings of the 1st International Conference on Wireless Internet*, pp. 114–121, 2005.
- [74] H. Mahboubi, W. Masoudimansour, A. G. Aghdam, and K. Sayrafian-Pour, “An energy-efficient target tracking strategy for mobile sensor networks in the presence of obstacles,” *Concordia University Technical Report*, 2012 (available online at www.ece.concordia.ca/~aghdam/TechnicalReports/techrep2012_2.pdf).
- [75] D. P. Bertsekas, *Nonlinear programming*. Athena scientific optimization and computation series, Athena Scientific, 1999.

- [76] H. Mahboubi, W. Masoudimansour, A. G. Aghdam, and K. Sayrafian-Pour, “Maximum life span strategy for target tracking in mobile sensor networks,” in *Proceedings of the American Control Conference*, pp. 5096–5101, 2012.